PHYSICAL REVIEW D **93,** 034035 (2016)

Properties of excited charm and charm-strange mesons

Stephen Godfrey* and Kenneth Moats

Department of Physics, Ottawa-Carleton Institute for Physics, Carleton University, Ottawa, Ontario K1S 5B6, Canada

(Received 2 December 2015; published 23 February 2016)

We calculate the properties of excited charm and charm-strange mesons. We use the relativized quark model to calculate their masses and wave functions that are used to calculate radiative transition partial widths and the $^3P_0$ quark-pair-creation model to calculate their strong decay widths. We use these results to make quark model spectroscopic assignments for recently observed charm and charm-strange mesons. In particular, we find that the properties of the $D_J(2550)^0$ and $D_J^*(2600)^0$ are consistent with those of the $2^1S_0(c\bar{u})$ and the $2^3S_1(c\bar{u})$ states respectively, and the $D_1^*(2760)^0$, $D_3^*(2760)^-$, and $D_J(2750)^0$ with those of the $1^3D_1(c\bar{u})$, $1^3D_3(d\bar{c})$, and $1D_2(c\bar{u})$ states respectively. We tentatively identify the $D_J^*(3000)^0$ as the $1^3F_4(c\bar{u})$ and favor the $D_J(3000)^0$ to be the $3^1S_0(c\bar{u})$ although we do not rule out the $1F_3$ and $1F_3'$ assignment. For the recently observed charm-strange mesons we identify the $D_{s1}^*(2709)^{\pm}$, $D_{s1}^*(2860)^-$, and $D_{s3}^*(2860)^-$ as the $2^3S_1(c\bar{s})$, $1^3D_1(s\bar{c})$, and $1^3D_3(s\bar{c})$ states respectively and suggest that the $D_{sJ}(3044)^{\pm}$ is most likely the $D_{s1}(2P_1')$ or $D_{s1}(2P_1)$ state although it might be the $D_{s2}^*(2^3P_2)$ with the DK final state too small to be observed with current statistics. Based on the predicted properties of excited states, that they do not have too large a total width and that they have a reasonable branching ratio to simple final states, we suggest states that should be able to be found in the near future. We expect that the tables of properties summarizing our results will be useful for interpreting future observations of charm and charm-strange mesons.

DOI: 10.1103/PhysRevD.93.034035

I. INTRODUCTION

Over the last decade, charm meson spectroscopy has undergone a resurgence due to the discovery of numerous excited charm and charm-strange states by the B-Factory experiments *BABAR* and Belle [1–7] and by the CLEO experiment [8]. More recently the LHCb experiment has demonstrated the capability of both observing these states and determining their properties [9–14]. This has led to considerable theoretical interest in attempting to make quark model spectroscopic assignments for these new states by comparing theoretical predictions to experimental measurements [15–32]. At the same time, steady progress is being made in lattice QCD [33–35] for which these experimental results and spectroscopic classifications are an important benchmark. With the start of higher energy and higher luminosity beams at the LHC and higher luminosity at the SuperKEKB e^+e^- collider we expect that more new states will be observed. To identify newly discovered states, a theoretical roadmap is needed. The quark model has been successful in taking on this role and we turn to it to calculate the properties of excited charm and charm-strange mesons.

An important property of heavy-light mesons is that in the limit that the heavy quark mass becomes infinite the properties of the meson are determined by those of the light quark [36–38]. The light quarks are characterized by their total angular momentum j_q such that $\vec{j}_q = \vec{s}_q + \vec{L}$ where s_q is the light quark spin and L is its orbital angular momentum. j_q is combined with S_Q, the spin of the heavy quark, to give the total angular momentum of the meson. The quantum numbers S_Q and j_q are separately conserved. Thus, for a given L, the states are grouped into doublets characterized by the angular momentum of the light quark. For example, the four $L = 1$ P-wave mesons can be grouped into two doublets characterized by the angular momentum of the light quark $j_q = 3/2$ with $J^P = 1^+, 2^+$ and $j_q = 1/2$ with $J^P = 0^+, 1^+$ where J and P are the total angular momentum and parity of the excited meson. In the heavy quark limit (HQL) the members of the doublets will be degenerate in mass, and this degeneracy is broken by $1/m_Q$ corrections [38,39]. For the $L = 1$ multiplet, heavy quark symmetry and conservation of parity and j_q also predict that the strong decays $D_{(s)J}^{(*)}(j_q = 3/2) \to D^{(*)}\pi(K)$ will only proceed through a D wave while the decays $D_{(s)J}^{(*)}(j_q = 1/2) \to D^{(*)}\pi(K)$ will only proceed via an S wave [40,41]. The states decaying to a D wave are expected to be narrow due to the angular momentum barrier while those decaying to an S wave are expected to be broad. Similar patterns are predicted for higher L multiplets so that measuring the properties of excited charm mesons can be used to both help identify them and to see how well excited states are described by the properties expected in the heavy quark limit. However, for higher mass states more phase space is available, leading to more possible decay channels,

*godfrey@physics.carleton.ca

resulting in more complicated decay patterns so that the predictions of the HQL are less apparent.

Our goals for this paper are twofold. First we want to provide a roadmap of charm and charm-strange meson properties to identify which states are the most promising candidates to be observed and the final states they are most likely to be observed in. Hereafter, for conciseness, we generally refer to both charm and charm-strange mesons as charm mesons. Second, when new states are observed we can use our roadmap to make quark model spectroscopic assignments for these newly found states.

In the first part of this paper we calculate the masses and wave functions of excited charm and charm-strange mesons using the relativized quark model [42] which we describe in the next section. Radiative transitions are described in Sec. III and strong decay widths are calculated using the $^3P_0$ quark-pair creation model [43,44] which is described in Sec. IV. These models have been described extensively in the literature so rather than repeating detailed descriptions of these models we give brief summaries and refer the interested reader to the references for further details. The outcome of this part of the paper is a comprehensive summary of excited charm meson properties.

In the second part, in Secs. V–VI, we use these results to examine the numerous newly observed charm and charm-strange mesons and attempt to make quark model spectroscopic assignments. This approach has been used in numerous papers although in some cases different calculations come to different conclusions. Thus, another goal of this paper is to suggest further diagnostic measurements that can resolve these differences to give an unambiguous spectroscopic assignment. In Sec. VII we use the quark model roadmap we produced in the first part of this paper to suggest which missing states, because of their properties, are most likely to be observed in the near future and suggest the most promising final states to study. We summarize our conclusions in the final section.

II. SPECTROSCOPY

We use the relativized quark model [42] (see also Ref. [45–48]) to calculate meson masses and their wave functions which we use to calculate decay properties. The model is described in detail in Ref. [42] to which we direct the interested reader. The general characteristics of this model are that it assumes a relativistic kinetic energy term and the potential incorporates a Lorentz vector one-gluon-exchange interaction with a QCD motivated running coupling constant, $\alpha_s(r)$, and a Lorentz scalar linear confining interaction. This is typical of most such models which are based on some variant of the Coulomb plus linear potential expected from QCD and that often include some relativistic effects [20,49–55]. The relativized quark model has been reasonably successful in describing most known mesons and has proven to be a useful guide to understanding newly found states [31,41,56–59]. However in recent years, starting with the discovery of the $D_{sJ}(2317)$ [8,60,61] and $X(3872)$ states [62], an increasing number of states have been observed that do not fit into this picture [63–66] pointing to the need to include physics which has hitherto been neglected such as coupled channel effects [67] which appear to be most important for states lying near kinematic thresholds. As a consequence of neglecting coupled channel effects and the crudeness of the relativization procedure we do not expect the mass predictions to be accurate to better than ~10–20 MeV.

For the case of a quark and antiquark of unequal mass, charge conjugation parity is no longer a good quantum number so that states with different total spins but with the same total angular momentum, such as the $^3P_1 - {}^1P_1$ and $^3D_2 - {}^1D_2$ pairs, can mix via the spin orbit interaction or some other mechanism. Consequently, the physical $J = 1$ P-wave states are linear combinations of $^3P_1$ and $^1P_1$ which we describe by

$$\begin{aligned} P &= {}^1P_1 \cos\theta_{nP} + {}^3P_1 \sin\theta_{nP} \\ P' &= -{}^1P_1 \sin\theta_{nP} + {}^3P_1 \cos\theta_{nP} \end{aligned} \tag{1}$$

where $P \equiv L = 1$ designates the relative angular momentum of the $c\overline{q}$ pair and the subscript $J = 1$ is the total angular momentum of the $c\overline{q}$ pair which is equal to L, and q can represent either a u, d or s quark. There are analogous expressions for higher L states where $L = D$, F, etc. Our notation implicitly implies $L - S$ coupling between the quark spins and the relative orbital angular momentum. In the heavy quark limit in which the heavy quark mass $m_Q \to \infty$, the states can be described by the total angular momentum of the light quark, j_q, which couples to the spin of the heavy quark and corresponds to $j - j$ coupling. In this limit the mixed states are given by [68]

$$\begin{aligned} \left|J = L, j_q = L + \frac{1}{2}\right\rangle &= \sqrt{\frac{J+1}{2J+1}}|J = L, S = 0\rangle \\ &\quad + \sqrt{\frac{J}{2J+1}}|J = L, S = 1\rangle \\ \left|J = L, j_q = L - \frac{1}{2}\right\rangle &= -\sqrt{\frac{J}{2J+1}}|J = L, S = 0\rangle \\ &\quad + \sqrt{\frac{J+1}{2J+1}}|J = L, S = 1\rangle. \end{aligned} \tag{2}$$

The $j_q = L - \frac{1}{2}$ state that is mainly spin triplet corresponds to the primed state in Eq. (1) and the $j_q = L + \frac{1}{2}$ that is mainly spin singlet corresponds to the unprimed state. For $L = 1$ the HQL gives rise to two doublets, one with $j_q = 1/2$ and the other with $j_q = 3/2$ and with the conventions of Eqs. (1)–(2) corresponds to $\theta_P = \tan^{-1}(-1/\sqrt{2}) \simeq -35.3°$. For $L = 2$ the HQL gives two doublets with $j_q = 3/2$ and $5/2$ with mixing angle $\theta_D = -\tan^{-1}(\sqrt{2/3}) = -39.2°$. The minus signs arise from our $c\overline{q}$ convention. Some authors prefer to use the $j - j$ basis [69] but since we solve our Hamiltonian equations

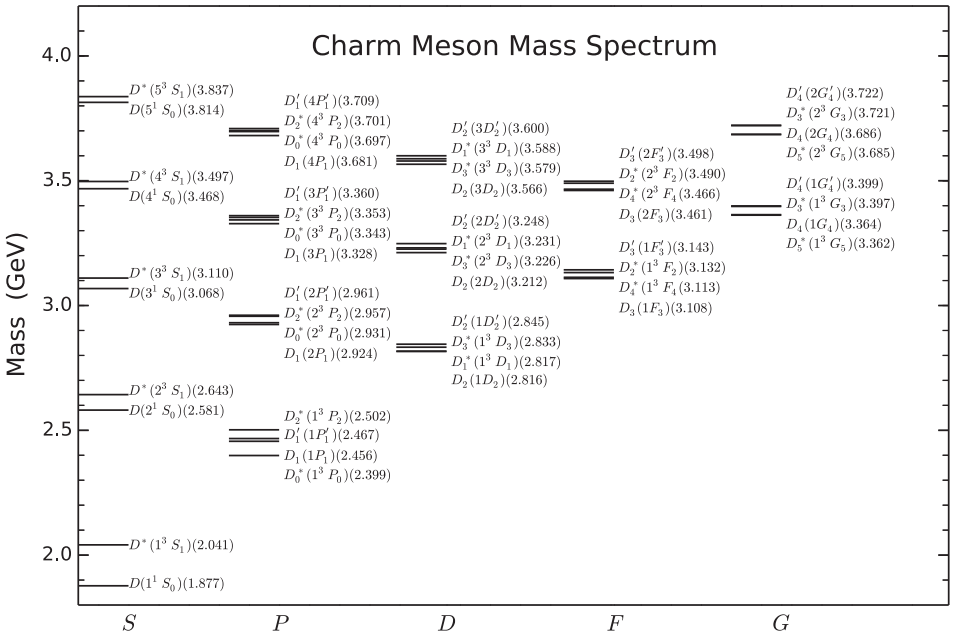

FIG. 1. The charm meson mass spectrum as predicted by the relativized quark model [42]. The ${}^3L_L - {}^1L_L$ mixing angles are given in Tables I–II.

assuming $L - S$ eigenstates and then include the LS mixing we use the notation of Eq. (1). Radiative transitions are sensitive to the ${}^3L_L - {}^1L_L$ mixing angle. We note that the definition of the mixing angles is fraught with ambiguities. For example, charge conjugating $c\overline{q}$ into $q\overline{c}$ flips the sign of the angle and the phase convention depends on the order of coupling $\vec{L}$, $\vec{S}_q$ and $\vec{S}_{\overline{q}}$ [70].

To solve the Hamiltonian to obtain masses and wave functions we used the following parameters: the slope of the linear confining potential is 0.18 GeV^2, $m_q = 0.22$ GeV, $m_s = 0.419$ GeV and $m_c = 1.628$ GeV. The predictions of our model for the charm mesons are given in Fig. 1 and for the charm-strange mesons in Fig 2; and the predicted masses and ${}^3L_L - {}^1L_L$ mixing angles are given in Tables I–II.

III. RADIATIVE TRANSITIONS

Radiative transitions have the potential to give information that could help identify newly discovered states. They

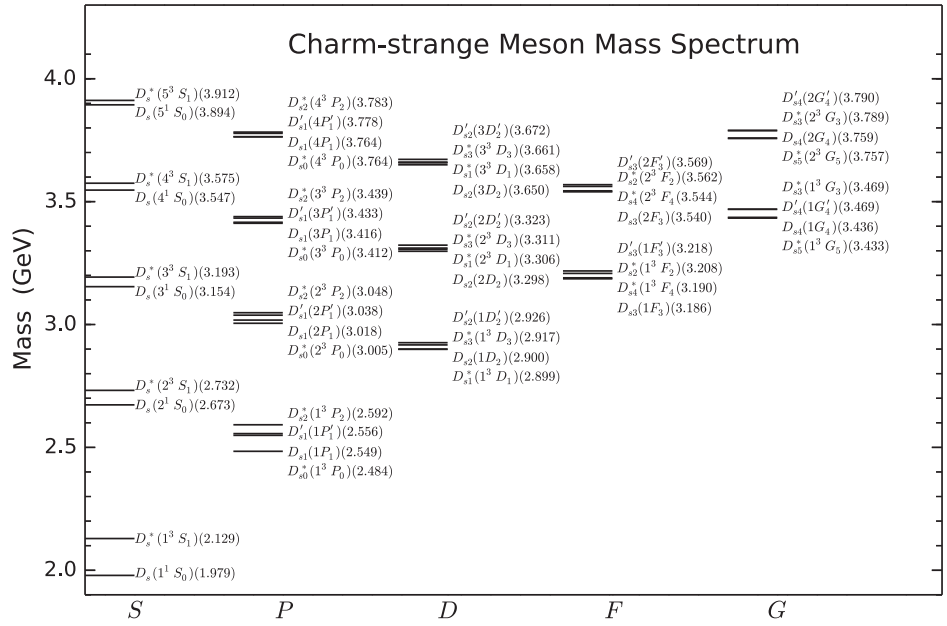

FIG. 2. The charm-strange meson mass spectrum as predicted by the relativized quark model [42]. The ${}^3L_L - {}^1L_L$ mixing angles are given in Tables I–II.

TABLE I. Predicted charm and charm-strange S- and P-wave meson masses, spin-orbit mixing angles and $\beta_{\rm eff}$'s. The $P_1 - P_1'$ states and mixing angles are defined using the convention of Eq. (1). Where two values of $\beta_{\rm eff}$ are listed, the first value is for the singlet state and the second value is for the triplet state.

	$c\bar{q}$		$c\bar{s}$	
State	Mass (MeV)	$\beta_{\rm eff}$ (GeV)	Mass (MeV)	$\beta_{\rm eff}$ (GeV)
1^3S_1	2041	0.516	2129	0.562
1^1S_0	1877	0.601	1979	0.651
2^3S_1	2643	0.434	2732	0.458
2^1S_0	2581	0.450	2673	0.475
3^3S_1	3110	0.399	3193	0.415
3^1S_0	3068	0.407	3154	0.424
4^3S_1	3497	0.382	3575	0.393
4^1S_0	3468	0.387	3547	0.400
5^3S_1	3837	0.371	3912	0.383
5^1S_0	3814	0.376	3894	0.393
1^3P_2	2502	0.437	2592	0.464
$1P_1$	2456	0.475, 0.482	2549	0.498, 0.505
$1P_1'$	2467	0.475, 0.482	2556	0.498, 0.505
1^3P_0	2399	0.516	2484	0.542
θ_{1P}	−25.68°		−37.48°	
2^3P_2	2957	0.402	3048	0.420
$2P_1$	2924	0.417, 0.419	3018	0.433, 0.434
$2P_1'$	2961	0.417, 0.419	3038	0.433, 0.434
2^3P_0	2931	0.431	3005	0.444
θ_{2P}	−29.39°		−30.40°	
3^3P_2	3353	0.383	3439	0.396
$3P_1$	3328	0.392, 0.392	3416	0.404, 0.404
$3P_1'$	3360	0.392, 0.392	3433	0.404, 0.404
3^3P_0	3343	0.398	3412	0.409
θ_{3P}	−28.10°		−27.72°	
4^3P_2	3701	0.371	3783	0.382
$4P_1$	3681	0.378, 0.377	3764	0.387, 0.387
$4P_1'$	3709	0.378, 0.377	3778	0.387, 0.387
4^3P_0	3697	0.381	3764	0.390
θ_{4P}	−26.91°		−25.43°	

TABLE II. Predicted charm and charm-strange D-, F-, and G-wave meson masses, spin-orbit mixing angles and $\beta_{\rm eff}$'s. The $D_2 - D_2'$, $F_3 - F_3'$ and $G_4 - G_4'$ states and mixing angles are defined using the convention of Eq. (1). Where two values of $\beta_{\rm eff}$ are listed, the first value is for the singlet state and the second value is for the triplet state.

	$c\bar{q}$		$c\bar{s}$	
State	Mass (MeV)	$\beta_{\rm eff}$ (GeV)	Mass (MeV)	$\beta_{\rm eff}$ (GeV)
1^3D_3	2833	0.407	2917	0.426
$1D_2$	2816	0.428, 0.433	2900	0.444, 0.448
$1D_2'$	2845	0.428, 0.433	2926	0.444, 0.448
1^3D_1	2817	0.456	2899	0.469
θ_{1D}	−38.17°		−38.47°	
2^3D_3	3226	0.385	3311	0.400
$2D_2$	3212	0.396, 0.399	3298	0.408, 0.410
$2D_2'$	3248	0.396, 0.399	3323	0.408, 0.410
2^3D_1	3231	0.410	3306	0.419
θ_{2D}	−37.44°		−37.71°	
3^3D_3	3579	0.372	3661	0.383
$3D_2$	3566	0.379, 0.381	3650	0.389, 0.390
$3D_2'$	3600	0.379, 0.381	3672	0.389, 0.390
3^3D_1	3588	0.387	3658	0.395
θ_{3D}	−36.90°		−37.15°	
1^3F_4	3113	0.390	3190	0.405
$1F_3$	3108	0.404, 0.407	3186	0.417, 0.419
$1F_3'$	3143	0.404, 0.407	3218	0.417, 0.419
1^3F_2	3132	0.423	3208	0.432
θ_{1F}	−39.52°		−39.30°	
2^3F_4	3466	0.374	3544	0.386
$2F_3$	3461	0.383, 0.385	3540	0.393, 0.394
$2F_3'$	3498	0.383, 0.385	3569	0.393, 0.394
2^3F_2	3490	0.394	3562	0.401
θ_{1F}	−39.38°		−39.12°	
1^3G_5	3362	0.379	3433	0.391
$1G_4$	3364	0.389, 0.391	3436	0.399, 0.401
$1G_4'$	3399	0.389, 0.391	3469	0.399, 0.401
1^3G_3	3397	0.402	3469	0.410
θ_{1G}	−40.18°		−39.95°	
2^3G_5	3685	0.367	3757	0.377
$2G_4$	3686	0.374, 0.375	3759	0.382, 0.383
$2G_4'$	3722	0.374, 0.375	3790	0.382, 0.383
2^3G_3	3721	0.383	3789	0.389
θ_{2G}	−40.23°		−39.93°	

are sensitive to the internal structure of states and can be particularly sensitive to ${}^3L_L - {}^1L_L$ mixing for states with $J = L$. However, in general, charm mesons lie above the Okubo-Zweig-Iizuka decay threshold so will have much larger strong decay partial widths than electromagnetic partial widths so in practice we expect the usefulness of electromagnetic transitions to be limited. Nevertheless, in this section we calculate electric dipole (E1) and magnetic dipole (M1) radiative widths. The partial width for an E1 radiative transition between states in the nonrelativistic quark model is given by [71]

$$\Gamma(\mathrm{n}^{2S+1}\mathrm{L}_J \to \mathrm{n}'^{2S'+1}\mathrm{L}'_{J'} + \gamma) = \frac{4}{3}\langle e_Q\rangle^2 \alpha k_\gamma^3 C_{fi}\delta_{SS'}\delta_{LL'\pm 1}|\langle \mathrm{n}'^{2S'+1}\mathrm{L}'_{J'}|r|\mathrm{n}^{2S+1}\mathrm{L}_J\rangle|^2, \quad (3)$$

where

$$\langle e_Q\rangle = \frac{m_c e_q - m_q e_{\bar{c}}}{m_q + m_c}. \quad (4)$$

$e_c = +2/3$ is the c-quark charge and q refers to the u, d and s quarks with charges $e_u = +2/3$, $e_d = -1/3$ and $e_s = -1/3$ respectively, in units of $|e|$, α is the fine-structure constant, k_γ is the photon's energy, and the angular momentum matrix element, C_{fi}, is given by

$$C_{fi} = \max(L, L')(2J' + 1)\begin{Bmatrix} L' & J' & S \\ J & L & 1 \end{Bmatrix}^2 \quad (5)$$

where $\{\cdots\}$ is a 6-j symbol. The matrix elements $\langle n'^{2S'+1}L'_{J'}|r|n^{2S+1}L_J\rangle$ were evaluated using the wave functions given by the relativized quark model [42]. Relativistic corrections are implicitly included in these E1 transitions through Siegert's theorem [72–74], by including spin-dependent interactions in the Hamiltonian used to calculate the meson masses and wave functions.

Radiative transitions which flip spin are described by M1 transitions. The rates for magnetic dipole transitions between S-wave states in heavy-light bound states are given in the nonrelativistic approximation by [75–77]

$$\Gamma(n^{2S+1}L_J \to n'^{2S'+1}L_{J'}+\gamma) = \frac{\alpha}{3}k_\gamma^3(2J'+1)\delta_{S,S'\pm1}|\langle f|\frac{e_q}{m_q}j_0\left(k_\gamma r\frac{m_{\bar{q}}}{m_q+m_{\bar{q}}}\right) - \frac{e_{\bar{q}}}{m_{\bar{q}}}j_0\left(k_\gamma r\frac{m_q}{m_q+m_{\bar{q}}}\right)|i\rangle|^2 \quad (6)$$

where e_q, the quark charges, and m_q, the quark masses, were given above, $L=0$ for S waves and $j_0(x)$ is the spherical Bessel function. Transitions in which the principle quantum number changes are referred to as hindered transitions as they are not allowed in the nonrelativistic limit due to the orthogonality of the wave functions. M1 transitions, especially hindered transitions, are notorious for their sensitivity to relativistic corrections [78]. In our calculations the wave function orthogonality is broken by including a smeared hyperfine interaction directly in the Hamiltonian so that the $^3S_1$ and $^1S_0$ states have slightly different wave functions.

The E1 and M1 radiative widths are given in Tables IV–XXVIII when they are large enough that they might be observed. More complete results are given in the Supplemental Material [79]. The tables in the supplementary material also include the matrix elements for the benefit of the interested reader. The predicted masses given in Tables I–II are used for all states. The photon energies were calculated using the predicted masses, but assuming these masses are all slightly shifted with respect to the measured masses, the phase space should remain approximately correct.

Given the sensitivity of radiative transitions to details of the models precise measurements of electromagnetic transition rates would provide stringent tests of the various calculations and predictions that have appeared in the literature.

IV. STRONG DECAYS

For states above the $D\pi$ and DK thresholds we calculate the strong decay widths of excited charm and charm-strange mesons using the $^3P_0$ quark-pair-creation model [43,44,57,58,80]. There are a number of predictions for charm meson widths in the literature using the $^3P_0$ model [19–24,55,81,82] and other models [15–17,39,49,83–85] but we believe that this work represents the most complete analysis of excited charm meson strong decays to date. The details of the notation and conventions used in our $^3P_0$ model calculations are given in the appendix of Ref. [86] to which we refer the interested reader.

We use the calculated charm and charm-strange meson masses listed in Tables I–II. For the light mesons we used the measured masses listed in Table III. For the charm and charm-strange mesons we use harmonic oscillator (HO) wave functions with the effective harmonic oscillator parameter, $\beta_{\rm eff}$, obtained by equating the rms radius of the harmonic oscillator wave function for the specified (n,l) quantum numbers to the rms radius of the wave functions calculated using the relativized quark model of Ref. [42]. A previous study [41] found that using HO wave functions with the fitted oscillator parameters gave results similar to those calculated using the exact relativized quark model wave functions but were far more computationally efficient. It was also found that the predictions of the $^3P_0$ model were similar to those of the flux-tube breaking model [87] when using the same wave functions in both calculations [41,58,88]. The widest variation in results occurs going from using either the exact relativized quark model wave functions or HO wave functions with $\beta_{\rm eff}$'s to using constant β's for all states [41] (compare also the results from Ref. [86] to those of Ref. [89]). This is because the decay amplitudes are dominated by the overlap of the three meson wave functions and the HO wave functions with $\beta_{\rm eff}$'s are a good representation of the exact wave

TABLE III. Light meson masses and effective harmonic oscillator parameters, $\beta_{\rm eff}$, used in the calculation of strong decay widths. The experimental values of the masses are taken from the Particle Data Group (PDG) [7]. The input value of the π mass is the weighted average of the experimental values of the π^0 and $\pi^\pm$ masses, and similarly for the input values of the K and K^* masses. All effective β values are taken to be 0.4 for the light mesons.

Meson	State	$M_{\rm input}$ (MeV)	$M_{\rm exp}$ (MeV) [7]	$\beta_{\rm eff}$ (GeV)
π	1^1S_0	138.8877	$134.8766 \pm 0.0006(\pi^0)$, $139.57018 \pm 0.00035(\pi^\pm)$	0.4
η	1^1S_0	547.862	547.862 ± 0.018	0.4
η'	1^1S_0	957.78	957.78 ± 0.06	0.4
ρ	1^3S_1	775.26	775.26 ± 0.25	0.4
ω	1^3S_1	782.65	782.65 ± 0.12	0.4
ϕ	1^3S_1	1019.461	1019.461 ± 0.019	0.4
K	1^1S_0	494.888	$497.614 \pm 0.024(K^0)$, $493.677 \pm 0.016(K^\pm)$	0.4
K^*	1^3S_1	894.36	$895.81 \pm 0.19(K^{*0})$, $891.66 \pm 0.26(K^{*\pm})$	0.4

TABLE IV. Partial widths and branching ratios for strong and electromagnetic decays for the $1S$, $2S$ and $3S$ charm mesons. The initial state's mass is given in MeV and is listed below the state's name in column 1. We only show radiative transitions that are likely to be observed and likewise generally do not show strong decay modes which have BR $\lesssim 1\%$ although they are included in calculating the total width and are included in the Supplemental Material [79]. The matrix elements for radiative transitions are given in the Supplemental Material [79]. Details of the calculations are given in the text.

Initial state	Final state	Width (cu, cd) (MeV)	BR (cu, cd) (%)
D^*	$D\gamma$	0.106, 0.0108	45.9, 8.0
2041	$D\pi$	0.125	54.1, 92.1
	Total	0.231, 0.136	100
$D(2^3S_1)$	$D\gamma$	0.60, 0.10	0.6, 0.1
2643	$D\pi$	26.1	25.6
	$D\eta$	3.85	3.8
	$D^*\pi$	58.8	57.6
	$D^*\eta$	1.97	1.9
	$D(1P_1')\pi$	0.65	0.6
	D_sK	8.8	8.6
	D_s^*K	1.1	1.1
	Total	102	100
$D(2^1S_0)$	$D^*\pi$	79.7	99.3
2581	$D(1^3P_0)\pi$	0.49	0.6
	Total	80	100
$D(3^3S_1)$	$D\gamma$	0.66, 0.12	0.6, 0.1
3110	$D\pi$	3.21	3.1
	$D\rho$	0.85	0.8
	$D\eta$	0.34	0.3
	$D\omega$	0.25	0.2
	$D^*\pi$	5.6	5.4
	$D^*\rho$	3.4	3.2
	$D^*\omega$	1.3	1.3
	$D(2^1S_0)\pi$	8.0	7.7
	$D(2^3S_1)\pi$	18.1	17.5
	$D(1P_1)\pi$	18.2	17.6
	$D(1P_1)\eta$	0.73	0.7
	$D(1P_1')\pi$	1.1	1.0
	$D(1P_1')\eta$	0.9	0.9
	$D(1^3P_2)\pi$	24.3	23.5
	$D_s^*K^*$	6.47	6.3
	$D_s(1P_1')K$	5.1	4.9
	Total	103	100
$D(3^1S_0)$	$D^*\pi$	5.2	4.9
3068	$D^*\rho$	9.8	9.3
	$D^*\eta'$	1.2	1.2
	$D^*\omega$	3.5	3.3
	$D(2^3S_1)\pi$	26.6	25.0
	$D(1^3P_2)\pi$	45.6	43
	D_sK^*	2.4	2.2
	D_s^*K	2.4	2.3
	$D_s^*K^*$	3.4	3.2
	$D_s(1^3P_0)K$	4.0	3.8
	Total	106	100

functions for this purpose. The effective harmonic oscillator wave function parameters, $\beta_{\rm eff}$, used in our calculations are listed in Tables I–II. For the light mesons we use the universal value of $\beta_{\rm eff} = 0.4$ GeV given in Table III (see below for an additional comment). In our calculations we use the constituent quark masses $m_c = 1.628$ GeV, $m_s = 0.419$ GeV, and $m_q = 0.220$ GeV $(q = u, d)$. Finally, we use "relativistic phase space" as described in Ref. [58,80] and in the appendix of Ref. [86].

Typical values of the parameters $\beta_{\rm eff}$ and γ, the quark-pair creation amplitude of the $^3P_0$ model, are found from fits to light meson decays [55,58]. The predicted widths are fairly insensitive to the precise values used for $\beta_{\rm eff}$ provided γ is appropriately rescaled. However γ can vary as much as 30% and still give reasonable overall fits of light meson decay widths [55]. This can result in factor of two changes to predicted widths, both smaller or larger. In our calculations of D_s meson strong decay widths in [31], we used a value of $\gamma = 0.4$, which has also been found to give a good description of strong decays of charm mesons and charmonium [55,57]. This scaling of the value of γ in different meson sectors has been studied in [90]. The resulting strong decay widths are listed in Tables IV–XLIII although we only show decays that have branching ratios (BR) greater than ~1% or decays to simple final states such as $D\pi$ or DK that might be easier to observe. More complete tables of results are given in the Supplemental Material [79].

V. CLASSIFICATION OF THE OBSERVED CHARM MESONS

The Belle, *BABAR* and LHCb collaborations have increased our knowledge of charm mesons considerably in recent years which has spawned a large number of theory papers attempting to categorize these new states. We list these new states and their properties in Table XLIV.

The $1P$ multiplet is well established and its measured properties agree well with theoretical expectations. Theory expects in the heavy quark limit two doublets, the $j = 1/2$ doublet composed of a 0^+ and 1^+ state, corresponding to the $D_0(2400)$ and $D_1(2430)$ states, that decay via S wave and are broad, and the $j = 3/2$ doublet composed of a 1^+ and 2^+ state, corresponding to the $D_1(2420)$ and the $D_2^*(2460)$ that decay via D wave and are relatively narrow. These states have been discussed in the literature (see for example [48]).

It is the large number of newly observed states that concerns us here. Given the success of quark model calculations in describing the $1P$ states we use the quark model predictions of the previous sections to classify these new states. The success of these efforts can be used to gauge the reliability of our predictions for the properties of undiscovered states. These states have been discussed in numerous papers [16,17,20–29,84,91–98].

TABLE V. Partial widths and branching ratios for strong and electromagnetic decays for the 4S charm mesons. See the caption to Table IV for further explanations.

Initial state	Final state	Width (cu, cd) (MeV)	BR (cu, cd) (%)
$D(4^3S_1)$ 3497	$D\gamma$	0.64, 0.12	0.45, 0.08
	$D(2^1S_0)\gamma$	0.43, 0.09	0.30, 0.06
	$D(3^1S_0)\gamma$	0.15, 0.03	0.11, 0.02
	$D\pi$	0.7	0.5
	$D^*\pi$	1.4	1.0
	$D(2^1S_0)\pi$	2.0	1.4
	$D(2^1S_0)\rho$	3.4	2.4
	$D(2^3S_1)\pi$	4.2	2.9
	$D(2^3S_1)\rho$	24.1	17.0
	$D(2^3S_1)\omega$	8.0	5.6
	$D(3^1S_0)\pi$	3.1	2.2
	$D(3^3S_1)\pi$	7.3	5.1
	$D(1P_1)\pi$	2.0	1.4
	$D(1P_1)\rho$	1.5	1.1
	$D(1P_1')\rho$	1.3	0.9
	$D(1^3P_2)\pi$	2.3	1.6
	$D(1^3P_2)\rho$	10.2	7.2
	$D(1^3P_2)\omega$	3.6	2.5
	$D(2P_1)\pi$	13.4	9.5
	$D(2P_1')\pi$	1.3	0.9
	$D(2^3P_2)\pi$	16.1	11.4
	$D(1D_2)\pi$	9.5	6.7
	$D(1^3D_3)\pi$	10.7	7.6
	$D_s(2^3S_1)K$	1.5	1.1
	Total	142	100
$D(4^1S_0)$ 3468	$D\rho$	0.4	0.3
	$D^*\pi$	1.4	0.9
	$D(2^1S_0)\rho$	8.7	5.6
	$D(2^1S_0)\omega$	3.0	2.0
	$D(2^3S_1)\pi$	5.4	3.5
	$D(2^3S_1)\rho$	19.1	12.4
	$D(2^3S_1)\omega$	5.7	3.7
	$D(3^3S_1)\pi$	11.0	7.1
	$D(1P_1)\rho$	4.4	2.9
	$D(1P_1)\omega$	1.6	1.0
	$D(1P_1')\rho$	1.9	1.2
	$D(1^3P_2)\pi$	2.9	1.9
	$D(1^3P_2)\rho$	10.9	7.1
	$D(1^3P_2)\omega$	3.6	2.4
	$D(2^3P_2)\pi$	33.9	22.0
	$D(1^3D_3)\pi$	25.0	16.2
	$D_s(2^3S_1)K$	3.9	2.6
	$D_s(1P_1')K^*$	2.3	1.5
	$D_s(1^3P_2)K$	3.20	2.1
	Total	154	100

TABLE VI. Partial widths and branching ratios for strong and electromagnetic decays for the 5S charm mesons. See the caption of Table IV for further explanations.

Initial state	Final state	Width (cu, cd) (MeV)	BR (cu, cd) (%)
$D(5^3S_1)$ 3837	$D\gamma$	0.61, 0.1	0.45, 0.09
	$D(2^1S_0)\gamma$	0.56, 0.1	0.41, 0.08
	$D(3^1S_0)\gamma$	0.32, 0.07	0.24, 0.05
	$D(4^1S_0)\gamma$	0.10, 0.02	0.08, 0.2
	$D^*\pi$	1.0	0.7
	$D^*\rho$	0.7	0.5
	$D(3^3S_1)\pi$	2.8	2.1
	$D(4^1S_0)\pi$	1.5	1.1
	$D(4^3S_1)\pi$	3.5	2.6
	$D(2P_1)\pi$	2.9	2.1
	$D(2P_1)\rho$	6.9	5.0
	$D(2P_1)\omega$	2.4	1.7
	$D(2^3P_2)\pi$	3.3	2.5
	$D(2^3P_2)\rho$	19.0	14
	$D(2^3P_2)\omega$	6.1	4.5
	$D(3P_1)\pi$	7.4	5.4
	$D(3P_1')\pi$	1.3	1.0
	$D(3^3P_2)\pi$	8.9	6.5
	$D(1D_2)\rho$	1.7	1.2
	$D(1^3D_3)\rho$	5.8	4.32
	$D(1^3D_3)\omega$	2.0	1.5
	$D(2D_2)\pi$	10.7	7.9
	$D(2^3D_3)\pi$	10.7	7.9
	$D(1F_3)\pi$	4.4	3.2
	$D(1^3F_4)\pi$	4.5	3.3
	$D_s(3^3S_1)K$	2.8	2.0
	$D_s(2^3P_2)K$	1.7	1.3
	Total	136	100
$D(5^1S_0)$ 3814	$D(2^3S_1)\pi$	1.4	0.9
	$D(2^3S_1)\rho$	1.5	0.9
	$D(3^3S_1)\pi$	4.2	2.7
	$D(4^3S_1)\pi$	5.3	3.4
	$D(2P_1)\rho$	13.0	8.3
	$D(2P_1)\omega$	4.2	2.7
	$D(2^3P_2)\pi$	6.0	3.9
	$D(2^3P_2)\rho$	13.8	8.8
	$D(2^3P_2)\omega$	4.2	2.7
	$D(3^3P_0)\pi$	1.1	0.7
	$D(3^3P_2)\pi$	20.1	12.9
	$D(1D_2)\rho$	3.9	2.5
	$D(1^3D_3)\pi$	1.9	1.2
	$D(1^3D_3)\rho$	5.6	3.6
	$D(1^3D_3)\omega$	1.9	1.2
	$D(2^3D_3)\pi$	28.0	18.0
	$D(1^3F_4)\pi$	12.8	8.2
	$D_s(3^3S_1)K$	5.67	3.6
	$D_s(2^3P_2)K$	5.32	3.4
	$D_s(1^3D_3)K$	2.0	1.3
	Total	156	100

A. The $D_J(2550)^0$ and $D_J^*(2600)^0$ states

Both the *BABAR* [2] and LHCb [11] collaborations have reported states around 2550 and 2600 MeV whose

TABLE VII. Partial widths and branching ratios for strong and electromagnetic decays for the $1P$ charm mesons. See the caption of Table IV for further explanations.

Initial state	Final state	Width (cu, cd) (MeV)	BR (cu, cd) (%)
$D(1^3P_0)$	$D^*\gamma$	0.288, 0.030	0.187, 0.019
2399	$D\pi$	154	99.8, 99.9
	Total	154	100
$D(1P_1)$	$D\gamma$	0.640, 0.066	6.01, 0.661
2456	$D^*\gamma$	0.0828, 0.0086	0.778, 0.086
	$D^*\pi$	9.92	93.2, 99.2
	Total	10.64, 10.00	100
$D(1P_1')$	$D\gamma$	0.156, 0.0161	0.097, 0.001
2467	$D^*\gamma$	0.386, 0.0399	0.239, 0.025
	$D^*\pi$	161	99.6, 99.9
	Total	162, 161	100
$D(1^3P_2)$	$D^*\gamma$	0.592, 0.0612	2.58, 0.27
2502	$D\pi$	15.3	66.6, 68.2
	$D\eta$	0.107	0.466, 0.477
	$D^*\pi$	6.98	30.4, 31.1
	Total	23.0, 22.4	100

measured properties we list in Table XLIV. The only states expected to fall in this mass region are the $2^1S_0(c\overline{q})$ and $2^3S_1(c\overline{q})$ states.

Starting with the $D_J(2550)^0$, the masses reported by the two experiments are inconsistent at the 2σ level. However *BABAR* and LHCb measure the widths to be 130 and 178 MeV with large errors. Given the large measured widths we believe that the experiments are seeing the same state but that it is difficult to extract masses precisely. With this assumption we average the masses and widths to obtain $M(D_J(2550)^0) = 2559$ MeV and $\Gamma(D_J(2550)^0) = 154$ MeV but do not attempt to estimate uncertainties given the naivety of the averaging. In addition LHCb makes the point that extracting its parameters is complicated [11]. Both experiments identify the $D_J(2550)^0$ as the $2^1S_0(c\overline{q})$ state. We predict the mass and width of the $2^1S_0(c\overline{q})$ state to be 2581 and 80 MeV respectively. We note that we predict the 1^3S_1 mass to be 2041 MeV which is ~34 MeV greater than its observed mass so that if we rescale the $2^1S_0(c\overline{q})$ mass by this amount we obtain 2547 MeV which is consistent with the observed average value. The calculated width is significantly smaller than the average of the measured widths. However, due to both the uncertainty in the theoretical width predictions and the large uncertainty in the measured width we consider the agreement between theory and experiment to be acceptable and conclude that the $D_J(2550)^0$ is the $2^1S_0(c\overline{q})$ state.

TABLE VIII. Partial widths and branching ratios for strong decays for the $2P$ charm mesons. See the caption for Table IV for further explanations.

Initial state	Final state	Width (MeV)	BR (%)
$D(2^3P_0)$	$D\pi$	25.4	13.4
2931	$D\eta$	1.53	0.8
	$D\eta'$	4.94	2.6
	$D^*\rho$	32.0	16.8
	$D^*\omega$	10.2	5.4
	$D(2^1S_0)\pi$	18.6	9.8
	$D(1P_1)\pi$	96.1	50.6
	D_sK	0.76	0.4
	Total	190	100
$D(2P_1)$	$D\rho$	3.4	2.7
2924	$D\omega$	1.1	0.9
	$D^*\pi$	37.9	30.3
	$D^*\rho$	24.4	19.5
	$D^*\eta$	5.0	4.0
	$D^*\omega$	8.2	6.5
	$D(2^3S_1)\pi$	1.3	1.0
	$D(1^3P_0)\pi$	4.9	3.9
	$D(1P_1)\pi$	5.2	4.2
	$D(1P_1')\pi$	2.5	2.0
	$D(1^3P_2)\pi$	7.4	5.9
	D_sK^*	14.3	11.4
	D_s^*K	9.0	7.2
	Total	125	100
$D(2P_1')$	$D\rho$	18.8	8.9
2961	$D\omega$	6.11	2.9
	$D^*\pi$	21.6	10.2
	$D^*\rho$	23.3	11.0
	$D^*\omega$	7.3	3.5
	$D(2^3S_1)\pi$	20.9	9.9
	$D(1P_1)\pi$	15.9	7.5
	$D(1P_1')\pi$	5.3	2.5
	$D(1^3P_2)\pi$	82.3	38.9
	D_sK^*	4.0	1.9
	D_s^*K	4.4	2.1
	Total	212	100
$D(2^3P_2)$	$D\pi$	5.0	4.4
2957	$D\rho$	10.6	9.3
	$D\eta$	1.3	1.2
	$D\omega$	3.5	3.0
	$D^*\pi$	17.1	15.0
	$D^*\rho$	26.3	23.0
	$D^*\eta$	2.8	2.5
	$D^*\omega$	9.2	8.1
	$D(2^1S_0)\pi$	2.40	2.1
	$D(2^3S_1)\pi$	1.4	1.2
	$D(1P_1)\pi$	5.7	5.0
	$D(1P_1')\pi$	6.5	5.7
	$D(1^3P_2)\pi$	11.9	10.4
	D_sK	3.7	3.2
	D_s^*K	5.6	4.9
	Total	114	100

TABLE IX. Partial widths and branching ratios for strong decays for the 3^3P_0 and $3P_1$ charm mesons. See the caption for Table IV for further explanations.

Initial state	Final state	Width (MeV)	BR (%)
$D(3^3P_0)$	$D\pi$	5.57	3.40
3343	$D\eta$	0.478	0.292
	$D^*\rho$	0.327	0.200
	$D(2^1S_0)\pi$	11.3	6.90
	$D(3^1S_0)\pi$	5.40	3.30
	$D(1^3P_0)\rho$	2.04	1.25
	$D(1P_1)\pi$	7.90	4.82
	$D(1P_1)\rho$	6.59	4.02
	$D(1P_1)\omega$	2.21	1.35
	$D(1P_1')\rho$	8.92	5.45
	$D(1P_1')\omega$	2.94	1.80
	$D(1^3P_2)\rho$	3.51	2.14
	$D(2P_1)\pi$	44.8	27.4
	$D(2P_1')\pi$	0.289	0.176
	$D(1D_2)\pi$	43.5	26.6
	$D_s^*K^*$	2.70	1.65
	$D_s(2^1S_0)K$	3.54	2.16
	$D_s(1P_1)K$	6.95	4.24
	$D_s(1P_1')K$	1.28	0.782
	Total	163.8	100
$D(3P_1)$	$D\rho$	1.02	0.848
3328	$D\omega$	0.318	0.264
	$D^*\pi$	4.54	3.78
	$D^*\rho$	0.299	0.25
	$D(2^3S_1)\pi$	15.2	12.6
	$D(2^3S_1)\eta$	1.88	1.56
	$D(1P_1)\rho$	17.8	14.8
	$D(1P_1)\omega$	5.85	4.86
	$D(1P_1')\rho$	7.71	6.41
	$D(1P_1')\omega$	2.49	2.07
	$D(1^3P_2)\pi$	20.5	17.0
	$D(1^3P_2)\rho$	5.52	4.59
	$D(1^3P_2)\eta$	2.14	1.78
	$D(1^3P_2)\omega$	1.58	1.31
	$D(2^3P_0)\pi$	2.54	2.11
	$D(2P_1)\pi$	2.61	2.17
	$D(2P_1')\pi$	1.02	0.848
	$D(2^3P_2)\pi$	5.56	4.62
	$D(1D_2)\pi$	3.11	2.59
	$D(1^3D_3)\pi$	6.44	5.36
	$D_s(2^3S_1)K$	2.42	2.01
	$D_s(1^3P_2)K$	3.03	2.52
	Total	120.2	100

We follow the same logic in comparing the measured properties of the $D_J^*(2600)^0$ to the predicted properties for the $2^3S_1(c\overline{q})$. Again the masses reported by *BABAR* and LHCb for the $D_J^*(2600)^0$ are incompatible at the level of 2σ and the measured widths are 93 and 140 MeV respectively

TABLE X. Partial widths and branching ratios for strong decays for the $3P_1'$ and 3^3P_2 charm mesons. See the caption for Table IV for further explanations.

Initial state	Final state	Width (MeV)	BR (%)
$D(3P_1')$	$D\rho$	1.85	0.986
3360	$D\omega$	0.595	0.317
	$D^*\pi$	4.54	2.42
	$D^*\rho$	0.746	0.398
	$D(2^1S_0)\rho$	3.81	2.03
	$D(2^3S_1)\pi$	11.1	5.92
	$D(3^3S_1)\pi$	6.11	3.26
	$D(1P_1)\rho$	6.73	3.59
	$D(1P_1)\omega$	2.18	1.16
	$D(1P_1')\rho$	6.00	3.20
	$D(1P_1')\omega$	2.03	1.08
	$D(1^3P_2)\pi$	7.28	3.88
	$D(1^3P_2)\rho$	11.3	6.02
	$D(1^3P_2)\omega$	3.53	1.88
	$D(2P_1)\pi$	7.70	4.10
	$D(2P_1')\pi$	2.20	1.17
	$D(2^3P_2)\pi$	35.2	18.8
	$D(1D_2)\pi$	11.0	5.86
	$D(1^3D_3)\pi$	37.9	20.2
	$D_s(2^3S_1)K$	7.40	3.94
	$D_s(1^3P_2)K$	7.70	4.10
	Total	187.6	100
$D(3^3P_2)$	$D\pi$	0.981	0.843
3353	$D\rho$	1.21	1.04
	$D\eta$	0.185	0.159
	$D\omega$	0.396	0.340
	$D^*\pi$	2.80	2.41
	$D(2^1S_0)\pi$	2.71	2.33
	$D(2^1S_0)\eta$	1.10	0.946
	$D(2^3S_1)\pi$	6.91	5.94
	$D(2^3S_1)\eta$	1.37	1.18
	$D(1P_1)\pi$	5.18	4.45
	$D(1P_1)\rho$	2.76	2.37
	$D(1P_1')\pi$	1.44	1.24
	$D(1P_1')\rho$	4.86	4.18
	$D(1P_1')\omega$	1.64	1.41
	$D(1^3P_2)\pi$	7.13	6.13
	$D(1^3P_2)\rho$	25.8	22.2
	$D(1^3P_2)\omega$	8.19	7.04
	$D(2P_1)\pi$	4.75	4.08
	$D(2P_1')\pi$	3.36	2.89
	$D(2^3P_2)\pi$	6.47	5.56
	$D(1D_2)\pi$	3.36	2.89
	$D(1^3D_3)\pi$	6.92	5.95
	$D_s(2^1S_0)K$	2.28	1.96
	$D_s(2^3S_1)K$	2.02	1.74
	$D_s(1P_1)K$	1.43	1.23
	$D_s(1^3P_2)K$	1.82	1.56
	Total	116.3	100

TABLE XI. Partial widths and branching ratios for strong decays for the 4^3P_0 and $4P_1$ charm mesons. See the caption for Table IV for further explanations.

Initial state	Final state	Width (MeV)	BR (%)
$D(4^3P_0)$	$D\pi$	1.93	1.21
3697	$D\eta$	0.219	0.137
	$D^*\rho$	0.450	0.282
	$D(2^1S_0)\pi$	3.20	2.01
	$D(2^3S_1)\rho$	2.74	1.72
	$D(3^1S_0)\pi$	5.41	3.39
	$D(4^1S_0)\pi$	2.59	1.63
	$D(1P_1)\pi$	1.78	1.12
	$D(2P_1)\pi$	11.7	7.34
	$D(3P_1)\pi$	20.2	12.7
	$D(1D_2)\pi$	3.20	2.01
	$D(1D_2)\rho$	4.46	2.80
	$D(2D_2)\pi$	38.2	24.0
	$D(2D_2')\pi$	0.949	0.595
	$D(1F_3)\pi$	19.7	12.4
	$D_s(2^3S_1)K^*$	2.43	1.52
	$D_s(3^1S_0)K$	10.4	6.53
	$D_s(1^3P_2)K^*$	1.64	1.03
	$D_s(2P_1)K$	10.0	6.27
	$D_s(1D_2)K$	4.22	2.65
	Total	159.4	100
$D(4P_1)$	$D\rho$	0.678	0.668
3681	$D^*\pi$	1.08	1.06
	$D(2^3S_1)\pi$	3.61	3.56
	$D(2^3S_1)\rho$	2.60	2.56
	$D(3^3S_1)\pi$	6.96	6.86
	$D(1^3P_2)\pi$	2.75	2.71
	$D(2^3P_0)\pi$	1.10	1.08
	$D(2^3P_2)\pi$	14.4	14.2
	$D(2^3P_2)\eta$	1.86	1.83
	$D(3^3P_0)\pi$	1.30	1.28
	$D(3P_1)\pi$	1.13	1.11
	$D(3^3P_2)\pi$	3.50	3.45
	$D(1D_2)\rho$	6.58	6.49
	$D(1D_2)\omega$	1.98	1.95
	$D(1D_2')\rho$	1.16	1.14
	$D(1^3D_3)\pi$	9.16	9.03
	$D(1^3D_3)\rho$	1.73	1.71
	$D(1^3D_3)\eta$	1.06	1.05
	$D(2D_2)\pi$	2.74	2.70
	$D(2^3D_3)\pi$	8.18	8.06
	$D(1F_3)\pi$	1.41	1.39
	$D(1^3F_4)\pi$	4.61	4.54
	$D_s(2^3S_1)K^*$	1.47	1.45
	$D_s(2^3P_0)K$	1.19	1.17
	$D_s(2^3P_2)K$	2.58	2.54
	$D_s(1^3D_3)K$	1.56	1.54
	Total	101.4	100

TABLE XII. Partial widths and branching ratios for strong decays for the $4P_1'$ and 4^3P_2 charm mesons. See the caption for Table IV for further explanations.

Initial state	Final state	Width (MeV)	BR (%)
$D(4P_1')$	$D\rho$	0.635	0.368
3709	$D^*\pi$	1.62	0.939
	$D(2^3S_1)\pi$	3.19	1.85
	$D(3^3S_1)\pi$	5.72	3.31
	$D(4^3S_1)\pi$	2.69	1.56
	$D(2P_1)\pi$	1.90	1.10
	$D(2^3P_2)\pi$	9.30	5.39
	$D(3P_1)\pi$	3.39	1.96
	$D(3P_1')\pi$	1.19	0.690
	$D(3^3P_2)\pi$	15.6	9.04
	$D(1D_2)\rho$	2.53	1.47
	$D(1^3D_3)\pi$	3.42	1.98
	$D(1^3D_3)\rho$	4.88	2.83
	$D(2D_2)\pi$	9.60	5.56
	$D(2^3D_3)\pi$	29.3	17.0
	$D(1F_3)\pi$	5.55	3.22
	$D(1^3F_4)\pi$	16.9	9.79
	$D_s(2^3S_1)K^*$	1.77	1.03
	$D_s(3^3S_1)K$	11.9	6.90
	$D_s(2^3P_2)K$	9.13	5.29
	$D_s(1^3D_3)K$	3.82	2.21
	Total	172.6	100
$D(4^3P_2)$	$D^*\pi$	0.698	0.757
3701	$D(2^3S_1)\pi$	1.88	2.04
	$D(2^3S_1)\rho$	1.99	2.16
	$D(3^1S_0)\pi$	1.18	1.28
	$D(3^3S_1)\pi$	3.15	3.42
	$D(1^3P_2)\pi$	1.29	1.40
	$D(1^3P_2)\rho$	1.30	1.41
	$D(2P_1)\pi$	3.87	4.20
	$D(2P_1)\eta$	1.17	1.27
	$D(2P_1')\pi$	1.47	1.59
	$D(2^3P_2)\pi$	5.04	5.47
	$D(3P_1)\pi$	3.13	3.40
	$D(3P_1')\pi$	1.67	1.81
	$D(3^3P_2)\pi$	3.46	3.75
	$D(1D_2)\pi$	2.58	2.80
	$D(1D_2)\rho$	1.28	1.39
	$D(1^3D_3)\pi$	2.70	2.93
	$D(1^3D_3)\rho$	9.68	10.5
	$D(1^3D_3)\omega$	2.95	3.20
	$D(2D_2)\pi$	5.12	5.55
	$D(2D_2')\pi$	0.985	1.07
	$D(2^3D_3)\pi$	6.72	7.29
	$D(1F_3)\pi$	2.14	2.32
	$D(1^3F_4)\pi$	3.58	3.88
	$D_s(2^3S_1)K^*$	1.33	1.44
	$D_s(2P_1)K$	1.76	1.91
	$D_s(2P_1')K$	1.57	1.70
	$D_s(2^3P_2)K$	1.94	2.10
	Total	92.19	100

TABLE XIII. Partial widths and branching ratios for strong and electromagnetic decays for the $1D$ charm mesons. See the caption for Table IV for further explanations.

Initial state	Final state	Width (cu, cd) (MeV)	BR (cu, cd) (%)
$D(1^3D_1)$ 2817	$D(1^3P_0)\gamma$	0.521, 0.0538	0.223, 0.0231
	$D\pi$	53.6	23.0
	$D\rho$	19.8	8.5
	$D\eta$	10.1	4.3
	$D\omega$	6.3	2.7
	$D^*\pi$	29.3	12.5
	$D^*\eta$	4.00	1.7
	$D(1P_1)\pi$	76.4	32.7
	$D(1P_1')\pi$	2.1	0.9
	$D(1^3P_2)\pi$	0.6	0.3
	D_sK	22.8	9.8
	D_s^*K	7.4	3.2
	Total	234	100
$D(1D_2)$ 2816	$D(1P_1)\gamma$	0.642, 0.066	0.61, 0.064
	$D\rho$	61.2	58.2
	$D\omega$	19.6	18.7
	$D^*\pi$	21.2	20.2
	Total	105	100
$D(1D_2')$ 2845	$D\rho$	5.85	2.4
	$D^*\pi$	93.3	38.3
	$D^*\rho$	5.0	2.1
	$D^*\eta$	14.7	6.0
	$D(1^3P_2)\pi$	89.9	36.9
	D_s^*K	29.5	12.1
	Total	244	100
$D(1^3D_3)$ 2833	$D(1^3P_2)\gamma$	0.69, 0.07	1.34, 0.14
	$D\pi$	20.1	39.2
	$D\rho$	1.30	2.5
	$D\eta$	1.24	2.4
	$D^*\pi$	15.5	30.2
	$D^*\rho$	7.56	14.8
	$D^*\omega$	1.1	2.2
	$D(1^3P_2)\pi$	0.9	1.8
	D_sK	1.1	2.20
	Total	51	100

TABLE XIV. Partial widths and branching ratios for strong decays for the 2^3D_1 and $2D_2$ charm mesons. See the caption for Table IV for further explanations.

Initial state	Final state	Width (MeV)	BR (%)
$D(2^3D_1)$ 3231	$D\pi$	11.0	5.14
	$D\rho$	1.33	0.621
	$D\eta$	1.23	0.575
	$D\omega$	0.418	0.195
	$D^*\pi$	4.41	2.06
	$D^*\rho$	29.7	13.9
	$D^*\omega$	9.73	4.54
	$D(2^1S_0)\pi$	6.07	2.84
	$D(2^1S_0)\eta$	2.53	1.18
	$D(2^3S_1)\pi$	4.37	2.04
	$D(1P_1)\pi$	25.3	11.8
	$D(1^3P_2)\pi$	14.8	6.91
	$D(2P_1)\pi$	18.3	8.55
	$D(1D_2)\pi$	53.7	25.1
	$D_s^*K^*$	3.14	1.47
	$D_s(2^1S_0)K$	4.17	1.95
	$D_s(1P_1)K$	12.0	5.61
	Total	214.1	100
$D(2D_2)$ 3212	$D\rho$	5.37	6.33
	$D\omega$	1.71	2.02
	$D^*\pi$	8.08	9.53
	$D^*\rho$	12.5	14.7
	$D^*\eta$	1.87	2.2
	$D^*\omega$	4.09	4.82
	$D(2^3S_1)\pi$	10.1	11.9
	$D(1^3P_0)\pi$	3.18	3.75
	$D(1P_1)\pi$	3.35	3.95
	$D(1P_1)\eta$	0.384	0.453
	$D(1P_1')\pi$	3.18	3.75
	$D(1^3P_2)\pi$	14.0	16.5
	$D(1D_2)\pi$	2.81	3.31
	D_s^*K	3.91	4.61
	$D_s^*K^*$	2.88	3.40
	$D_s(1^3P_0)K$	1.03	1.21
	Total	84.8	100

with large errors. Averaging the masses and widths measured by the two experiments we obtain $M(D_J^*(2600)^0) = 2629$ MeV and $\Gamma(D_J^*(2600)^0) = 117$ MeV and again we do not assign errors given the lack of justification for using simple averages. We predict the mass and width of the $2^3S_1(c\overline{q})$ state to be 2643 and 102 MeV respectively. Again, if we rescale the $2^3S_1(c\overline{q})$ mass down by 34 MeV we obtain 2609 MeV. Further, we find that $\Gamma(D^*(2S) \to D\pi)/\Gamma(D^*(2S) \to D^*\pi) = 0.44$ versus the *BABAR* [2] measurement of $0.32 \pm 0.02 \pm 0.09$. We conclude that the $D_J^*(2600)^0$ properties are consistent with the predicted properties of the $2^3S_1(c\overline{q})$.

To summarize, our results support the identification of the $D_J(2550)^0$ and $D_J^*(2600)^0$ with the $2^1S_0(c\overline{q})$ and $2^3S_1(c\overline{q})$ respectively made by the *BABAR* [2] and LHCb [11] collaborations and previous theoretical studies [23–26,32,91,97,98].

B. The $D_J(2750)^0$, $D_1^*(2760)^0$ and $D_3^*(2760)^0$ states

The *BABAR* [2] and LHCb [9–11] collaborations have observed a number of new states in the mass region of 2740 to 2800 MeV. They can be grouped into the unnatural parity $D_J(2750)$ seen in the $D^*\pi$ final state and some number of natural parity states collectively labeled the $D_J^*(2760)$ which has recently been resolved by LHCb into two states with $J^P = 1^-$ and 3^- labeled the $D_1^*(2760)$ [9] and $D_3^*(2760)$ [10] seen in the $D\pi$ final state. The states

TABLE XV. Partial widths and branching ratios for strong decays for the $2D_2'$ and 2^3D_3 charm mesons. See the caption for Table IV for further explanations.

Initial state	Final state	Width (MeV)	BR (%)
$D(2D_2')$ 3248	$D\rho$	5.89	2.71
	$D\omega$	1.97	0.907
	$D^*\pi$	17.0	7.83
	$D^*\rho$	15.9	7.32
	$D^*\eta$	1.38	0.636
	$D^*\eta'$	0.479	0.221
	$D^*\omega$	5.21	2.40
	$D(2^3S_1)\pi$	12.2	5.62
	$D(2^3S_1)\eta$	2.42	1.11
	$D(1P_1)\pi$	4.66	2.15
	$D(1P_1)\rho$	2.74	1.26
	$D(1P_1')\pi$	3.62	1.67
	$D(1^3P_2)\pi$	32.2	14.8
	$D(1^3P_2)\eta$	2.38	1.10
	$D(2^3P_2)\pi$	19.7	9.07
	$D(1D_2)\pi$	4.78	2.20
	$D(1^3D_3)\pi$	56.1	25.8
	$D_s^*K^*$	3.00	1.38
	$D_s(1^3P_2)K$	15.1	6.96
	Total	217.1	100
$D(2^3D_3)$ 3226	$D\rho$	1.96	2.69
	$D\eta$	0.108	0.148
	$D\eta'$	0.261	0.359
	$D^*\pi$	2.16	2.97
	$D^*\rho$	8.28	11.4
	$D^*\eta$	0.708	0.973
	$D^*\eta'$	0.321	0.441
	$D^*\omega$	2.63	3.62
	$D(2^1S_0)\pi$	7.24	9.95
	$D(2^3S_1)\pi$	6.82	9.38
	$D(1P_1)\pi$	8.68	11.9
	$D(1P_1')\pi$	5.20	7.15
	$D(1^3P_2)\pi$	10.7	14.7
	$D(1D_2')\pi$	1.12	1.54
	$D(1^3D_3)\pi$	3.53	4.85
	D_s^*K	1.71	2.35
	$D_s^*K^*$	3.74	5.14
	$D_s(1P_1')K$	1.30	1.79
	$D_s(1^3P_2)K$	0.900	1.24
	Total	72.7	100

predicted to be closest in mass to these states are the $1D$ states. The next nearest states are the $2P$ multiplet which is expected to lie in the 2900 to 2950 MeV mass region but whose quantum numbers are inconsistent with the recent LHCb measurements [9,10]. We therefore concentrate on the expected properties of the $1D$ multiplet. As we did for the $2S$ multiplet, for the purposes of comparing our mass predictions to the measured masses, we rescale our predictions down by the difference between predicted and measured masses for the $D^*(1S)$ state of 34 MeV.

TABLE XVI. Partial widths and branching ratios for strong decays for the 3^3D_1 and $3D_2$ charm mesons. See the caption for Table IV for further explanations.

Initial state	Final state	Width (MeV)	BR (%)
$D(3^3D_1)$ 3588	$D\pi$	2.99	1.47
	$D^*\pi$	1.12	0.551
	$D^*\rho$	2.33	1.15
	$D(2^1S_0)\pi$	3.77	1.86
	$D(2^3S_1)\pi$	2.21	1.09
	$D(2^3S_1)\rho$	15.1	7.43
	$D(2^3S_1)\omega$	4.74	2.33
	$D(1P_1)\pi$	4.24	2.09
	$D(1^3P_2)\rho$	13.3	6.55
	$D(1^3P_2)\omega$	4.26	2.10
	$D(2P_1)\pi$	14.7	7.24
	$D(2^3P_2)\pi$	5.76	2.84
	$D(3P_1)\pi$	6.60	3.25
	$D(1D_2)\pi$	8.49	4.18
	$D(1^3D_3)\pi$	6.25	3.08
	$D(2D_2)\pi$	31.7	15.6
	$D(1F_3)\pi$	26.5	13.0
	$D_s(2P_1)K$	13.9	6.84
	$D_s(1D_2)K$	9.09	4.48
	Total	203.1	100
$D(3D_2)$ 3566	$D\rho$	2.01	2.11
	$D\omega$	0.653	0.684
	$D^*\pi$	1.74	1.82
	$D^*\rho$	1.49	1.56
	$D(2^1S_0)\rho$	0.970	1.02
	$D(2^3S_1)\pi$	2.93	3.07
	$D(2^3S_1)\rho$	8.69	9.11
	$D(2^3S_1)\eta$	1.55	1.62
	$D(2^3S_1)\omega$	2.86	3.00
	$D(3^3S_1)\pi$	4.79	5.02
	$D(1P_1)\rho$	1.79	1.88
	$D(1^3P_2)\pi$	4.38	4.59
	$D(1^3P_2)\rho$	6.20	6.50
	$D(1^3P_2)\eta$	1.09	1.14
	$D(1^3P_2)\omega$	2.03	2.13
	$D(2^3P_0)\pi$	1.73	1.81
	$D(2P_1)\pi$	1.76	1.84
	$D(2P_1')\pi$	1.49	1.56
	$D(2^3P_2)\pi$	13.5	14.1
	$D(1D_2)\pi$	2.03	2.13
	$D(1^3D_3)\pi$	8.65	9.06
	$D(2D_2)\pi$	1.97	2.06
	$D(1F_3)\pi$	1.75	1.83
	$D_s(2^3S_1)K$	3.86	4.04
	$D_s(1^3P_2)K$	1.88	1.97
	Total	95.4	100

Starting with the $D_3^*(2760)^0$ state, the measured mass and width from the LHCb isobar analysis are 2798 ± 10 and 105 ± 30 MeV [10] respectively where for simplicity we have combined the statistical, experimental and

TABLE XVII. Partial widths and branching ratios for strong decays for the $3D_2'$ and 3^3D_3 charm mesons. See the caption for Table IV for further explanations.

Initial state	Final state	Width (MeV)	BR (%)
$D(3D_2')$ 3600	$D^*\pi$	4.53	2.14
	$D^*\rho$	2.09	0.989
	$D(2^1S_0)\rho$	7.28	3.44
	$D(2^1S_0)\omega$	2.37	1.12
	$D(2^3S_1)\pi$	6.22	2.94
	$D(2^3S_1)\rho$	10.2	4.82
	$D(2^3S_1)\omega$	3.32	1.57
	$D(3^3S_1)\pi$	3.14	1.49
	$D(1P_1)\rho$	4.34	2.05
	$D(1^3P_2)\pi$	5.84	2.76
	$D(1^3P_2)\rho$	6.54	3.09
	$D(1^3P_2)\omega$	2.19	1.04
	$D(2^3P_2)\pi$	16.6	7.85
	$D(3^3P_2)\pi$	7.16	3.39
	$D(1D_2)\pi$	3.13	1.48
	$D(1^3D_3)\pi$	11.5	5.44
	$D(2D_2)\pi$	3.44	1.63
	$D(2^3D_3)\pi$	30.4	14.4
	$D(1F_3)\pi$	3.32	1.57
	$D(1^3F_4)\pi$	27.6	13.1
	$D_s(2^3P_2)K$	16.3	7.71
	$D_s(1^3D_3)K$	9.18	4.34
	Total	211.4	100
$D(3^3D_3)$ 3579	$D^*\pi$	0.645	0.716
	$D^*\rho$	2.62	2.91
	$D^*\omega$	0.835	0.926
	$D(2^1S_0)\rho$	3.32	3.68
	$D(2^1S_0)\omega$	1.07	1.19
	$D(2^3S_1)\pi$	0.798	0.885
	$D(2^3S_1)\rho$	8.09	8.98
	$D(2^3S_1)\omega$	2.87	3.18
	$D(3^1S_0)\pi$	3.42	3.79
	$D(3^3S_1)\pi$	3.27	3.63
	$D(1P_1)\rho$	1.74	1.93
	$D(1P_1')\pi$	1.36	1.51
	$D(1^3P_2)\pi$	1.76	1.95
	$D(1^3P_2)\rho$	5.21	5.78
	$D(1^3P_2)\omega$	1.81	2.01
	$D(2P_1)\pi$	9.40	10.4
	$D(2P_1')\pi$	2.74	3.04
	$D(2^3P_2)\pi$	7.50	8.32
	$D(1D_2)\pi$	4.40	4.88
	$D(1^3D_3)\pi$	4.92	5.46
	$D(2^3D_3)\pi$	2.42	2.68
	$D(1^3F_4)\pi$	2.36	2.62
	$D_s(2^1S_0)K$	1.36	1.51
	$D_s(2^3S_1)K$	1.96	2.17
	$D_s(1^3P_2)K^*$	1.23	1.36
	$D_s(1D_2')K$	0.960	1.07
	Total	90.13	100

TABLE XVIII. Partial widths and branching ratios for strong and electromagnetic decays for the $1F$ charm mesons. See the caption for Table IV for further explanations.

Initial state	Final state	Width (cu, cd) (MeV)	BR (cu, cd) (%)
$D(1^3F_2)$ 3132	$D(1^3D_1)\gamma$	0.70, 0.073	0.29, 0.03
	$D\pi$	23.1	9.5
	$D\rho$	16.4	6.7
	$D\eta$	4.4	1.8
	$D\omega$	5.4	2.2
	$D^*\pi$	18.5	7.6
	$D^*\rho$	16.0	6.6
	$D^*\eta$	3.15	1.3
	$D^*\omega$	5.1	2.1
	$D(1P_1)\pi$	52.9	21.7
	$D(1P_1)\eta$	6.60	2.7
	$D(1^3P_2)\pi$	10.3	4.2
	$D(1D_2)\pi$	43.8	18.0
	D_sK	7.92	3.2
	D_s^*K	5.11	2.1
	$D_s(1P_1)K$	9.5	3.9
	Total	243	100
$D(1F_3)$ 3108	$D(1D_2)\gamma$	0.73, 0.075	0.58, 0.060
	$D\rho$	38.9	31
	$D\omega$	12.9	10.2
	$D^*\pi$	25.1	20.0
	$D^*\rho$	25.6	20.3
	$D^*\omega$	8.27	6.6
	$D(1^3P_2)\pi$	1.93	1.5
	D_sK^*	4.10	3.3
	Total	126	100
$D(1F_3')$ 3143	$D(1D_2')\gamma$	0.74, 0.077	0.28, 0.0296
	$D\rho$	9.8	3.6
	$D\omega$	3.1	1.2
	$D^*\pi$	46.2	17.2
	$D^*\rho$	29.5	11.0
	$D^*\eta$	8.2	3.1
	$D^*\omega$	9.6	3.6
	$D(2^3S_1)\pi$	5.1	1.9
	$D(1^3P_2)\pi$	69.7	25.9
	$D(1^3P_2)\eta$	6.8	2.5
	$D(1^3D_3)\pi$	50.3	18.7
	D_s^*K	13.9	5.2
	$D_s(1^3P_2)K$	7.5	2.8
	Total	269	100
$D(1^3F_4)$ 3113	$D(1^3D_3)\gamma$	0.75, 0.077	0.58, 0.060
	$D\pi$	15.8	12.2
	$D\rho$	4.0	3.1
	$D\eta$	1.4	1.1
	$D^*\pi$	15.2	11.8
	$D^*\rho$	59.1	45.7
	$D^*\omega$	19.2	14.8
	$D(1P_1)\pi$	1.7	1.4
	$D(1^3P_2)\pi$	4.1	3.2
	Total	129	100

TABLE XIX. Partial widths and branching ratios for strong decays for the 2^3F_2 and $2F_3$ charm mesons. See the caption for Table IV for further explanations.

Initial state	Final state	Width (MeV)	BR (%)
$D(2^3F_2)$ 3490	$D\pi$	6.34	2.84
	$D\rho$	2.35	1.05
	$D^*\pi$	4.13	1.85
	$D^*\rho$	9.98	4.47
	$D^*\omega$	3.32	1.49
	$D(2^1S_0)\rho$	4.60	2.06
	$D(1^3P_0)\rho$	2.69	1.20
	$D(1P_1)\pi$	12.6	5.64
	$D(1P_1)\rho$	6.13	2.74
	$D(1P_1')\rho$	4.70	2.10
	$D(1^3P_2)\pi$	5.89	2.64
	$D(1^3P_2)\rho$	4.95	2.22
	$D(2P_1)\pi$	11.4	5.10
	$D(2^3P_2)\pi$	4.76	2.13
	$D(1D_2)\pi$	24.5	11.0
	$D(1D_2)\eta$	2.40	1.07
	$D(1^3D_3)\pi$	7.33	3.28
	$D(2D_2)\pi$	15.1	6.76
	$D(1F_3)\pi$	32.5	14.5
	$D_s(2^1S_0)K$	4.38	1.96
	$D_s(2^3S_1)K$	2.72	1.22
	$D_s(1D_2)K$	14.9	6.67
	Total	223	100
$D(2F_3)$ 3461	$D\rho$	6.37	5.96
	$D\omega$	2.08	1.95
	$D^*\rho$	5.51	5.16
	$D^*\omega$	1.81	1.69
	$D(2^1S_0)\rho$	7.67	7.18
	$D(2^1S_0)\omega$	2.30	2.15
	$D(2^3S_1)\pi$	15.4	14.4
	$D(2^3S_1)\rho$	1.16	1.09
	$D(1P_1)\rho$	7.23	6.77
	$D(1P_1)\omega$	2.50	2.34
	$D(1P_1')\pi$	1.38	1.29
	$D(1P_1')\rho$	3.40	3.18
	$D(1P_1')\omega$	1.07	1.00
	$D(1^3P_2)\pi$	14.2	13.3
	$D(1^3P_2)\rho$	5.55	5.20
	$D(1^3P_2)\omega$	1.81	1.69
	$D(2^3P_0)\pi$	1.08	1.01
	$D(2P_1)\pi$	1.99	1.86
	$D(2^3P_2)\pi$	1.61	1.51
	$D(1^3D_1)\pi$	1.71	1.60
	$D(1D_2)\pi$	3.33	3.12
	$D(1^3D_3)\pi$	2.36	2.21
	Total	106.8	100

systematic errors in quadrature. These values should be compared to the predicted mass (after rescaling) and width of the $1^3D_3(c\overline{q})$ state which are 2799 and 51 MeV respectively. The agreement between experiment and our

TABLE XX. Partial widths and branching ratios for strong decays for the $2F_3'$ and 2^3F_4 charm mesons. See the caption for Table IV for further explanations.

Initial state	Final state	Width (MeV)	BR (%)
$D(2F_3')$ 3498	$D^*\pi$	11.9	5.27
	$D^*\rho$	6.21	2.75
	$D(2^3S_1)\pi$	3.40	1.51
	$D(2^3S_1)\rho$	3.90	1.73
	$D(2^3S_1)\eta$	2.54	1.13
	$D(3^3S_1)\pi$	2.36	1.05
	$D(1P_1)\rho$	3.20	1.42
	$D(1P_1')\pi$	1.43	0.634
	$D(1P_1')\rho$	4.76	2.11
	$D(1^3P_2)\pi$	17.4	7.71
	$D(1^3P_2)\rho$	11.1	4.92
	$D(1^3P_2)\omega$	3.66	1.62
	$D(2P_1)\pi$	2.87	1.27
	$D(2^3P_2)\pi$	15.1	6.69
	$D(1D_2)\pi$	4.38	1.94
	$D(1^3D_3)\pi$	29.5	13.1
	$D(1^3D_3)\eta$	2.81	1.24
	$D(2^3D_3)\pi$	15.8	7.00
	$D(1^3F_4)\pi$	34.9	15.5
	$D_s(2^3S_1)K$	6.83	3.03
	$D_s(1^3P_2)K$	2.54	1.13
	$D_s(1^3D_3)K$	16.2	7.18
	Total	225.7	100
$D(2^3F_4)$ 3466	$D\pi$	0.829	0.849
	$D^*\rho$	8.98	9.20
	$D^*\eta'$	0.165	0.169
	$D^*\omega$	2.90	2.97
	$D(2^1S_0)\pi$	7.50	7.68
	$D(2^3S_1)\pi$	8.47	8.67
	$D(2^3S_1)\rho$	3.42	3.50
	$D(1^3P_0)\rho$	1.49	1.53
	$D(1P_1)\pi$	6.42	6.57
	$D(1P_1)\rho$	1.90	1.95
	$D(1P_1')\pi$	2.01	2.06
	$D(1P_1')\rho$	2.96	3.03
	$D(1^3P_2)\pi$	5.97	6.11
	$D(1^3P_2)\rho$	13.8	14.1
	$D(1^3P_2)\omega$	4.81	4.93
	$D(2P_1)\pi$	1.44	1.47
	$D(2P_1')\pi$	1.50	1.54
	$D(2^3P_2)\pi$	2.94	3.01
	$D(1D_2)\pi$	1.30	1.33
	$D(1D_2')\pi$	2.30	2.36
	$D(1^3D_3)\pi$	4.67	4.78
	$D(1^3F_4)\pi$	1.27	1.30
	$D_s(1P_1')K$	1.10	1.13
	$D_s(1^3P_2)K$	1.10	1.13
	Total	97.6	100

TABLE XXI. Partial widths and branching ratios for strong and electromagnetic decays for the 1^3G_3 and $1G_4$ charm mesons. See the caption for Table IV for further explanations.

Initial state	Final state	Width (cu, cd) (MeV)	BR (cu, cd) (%)
$D(1^3G_3)$ 3397	$D(1^3F_2)\gamma$	0.74, 0.076	0.32, 0.033
	$D\pi$	10.2	4.4
	$D\rho$	8.48	3.6
	$D\eta$	1.90	0.81
	$D\eta'$	1.6	0.7
	$D\omega$	2.82	1.2
	$D^*\pi$	9.7	4.1
	$D^*\rho$	19.4	8.3
	$D^*\omega$	6.3	2.7
	$D(2^1S_0)\pi$	5.6	2.4
	$D(2^3S_1)\pi$	3.5	1.5
	$D(1P_1)\pi$	30.7	13.1
	$D(1P_1)\rho$	11.9	5.1
	$D(1P_1)\eta$	5.6	2.4
	$D(1P_1)\omega$	3.7	1.6
	$D(1^3P_2)\pi$	11.3	4.8
	$D(2P_1)\pi$	5.4	2.3
	$D(1D_2)\pi$	36.6	15.6
	$D(1^3D_3)\pi$	3.6	1.6
	$D(1F_3)\pi$	24.6	10.5
	D_sK	2.6	1.1
	$D_s(1P_1)K$	9.3	4.0
	Total	234	100
$D(1G_4)$ 3364	$D(1F_3)\gamma$	0.76, 0.079	0.62, 0.064
	$D\rho$	18.5	15.0
	$D\omega$	6.2	5.0
	$D^*\pi$	20.3	16.5
	$D^*\rho$	21.0	17.0
	$D^*\eta$	1.8	1.5
	$D^*\omega$	6.9	5.6
	$D(2^3S_1)\pi$	1.5	1.2
	$D(1^3P_0)\pi$	2.1	1.7
	$D(1P_1)\pi$	2.9	2.3
	$D(1P_1)\rho$	18.8	15.2
	$D(1P_1)\omega$	5.7	4.6
	$D(1P_1')\pi$	2.0	1.7
	$D(1^3P_2)\pi$	4.2	3.4
	$D(1^3P_2)\rho$	2.2	1.8
	D_sK^*	2.1	1.7
	$D_s^*K^*$	1.3	1.1
	Total	123	100

TABLE XXII. Partial widths and branching ratios for strong and electromagnetic decays for the $1G_4'$ and 1^3G_5 charm mesons. See the caption for Table IV for further explanations.

Initial state	Final state	Width (cu, cd) (MeV)	BR (cu, cd) (%)
$D(1G_4')$ 3399	$D(1F_3')\gamma$	0.75, 0.078	0.30, 0.031
	$D\rho$	9.0	3.5
	$D\omega$	2.9	1.2
	$D^*\pi$	22.0	8.6
	$D^*\rho$	23.6	9.3
	$D^*\eta$	4.0	1.6
	$D^*\eta'$	2.45	1.0
	$D^*\omega$	7.8	3.0
	$D(2^3S_1)\pi$	9.2	3.6
	$D(1P_1)\pi$	3.4	1.4
	$D(1^3P_2)\pi$	43.2	17.0
	$D(1^3P_2)\rho$	11.1	4.4
	$D(1^3P_2)\eta$	7.6	3.0
	$D(1^3P_2)\omega$	3.3	1.3
	$D(2^3P_2)\pi$	5.6	2.2
	$D(1^3D_3)\pi$	43.9	17.2
	$D(1^3F_4)\pi$	28.2	11.1
	D_s^*K	5.4	2.1
	$D_s(1^3P_2)K$	11.9	4.7
	Total	254	100
$D(1^3G_5)$ 3362	$D(1^3F_4)\gamma$	0.78, 0.080	0.66, 0.068
	$D\pi$	10.0	8.4
	$D\rho$	3.9	3.3
	$D\eta$	1.0	0.9
	$D\omega$	1.2	1.1
	$D^*\pi$	11.2	9.5
	$D^*\rho$	38.3	32.4
	$D^*\omega$	12.6	10.6
	$D(2^1S_0)\pi$	1.3	1.1
	$D(1P_1)\pi$	3.0	2.6
	$D(1P_1')\pi$	2.8	2.3
	$D(1^3P_2)\pi$	6.2	5.2
	$D(1^3P_2)\rho$	13.1	11.1
	$D(1^3P_2)\omega$	3.7	3.1
	$D(1^3D_3)\pi5$	1.5	1.2
	$D_s^*K^*$	2.9	2.4
	Total	118	100

predictions for both the mass and total width are satisfactory so we identify the $D_3^*(2760)^0$ as the $1^3D_3(c\overline{q})$ state.

Similarly we compare the measured mass and width for the $D_1^*(2760)^0$ which are $M = 2781 \pm 22$ MeV and $\Gamma = 177 \pm 38$ MeV [9] where again we have combined the statistical, experimental and systematic errors in quadrature. The predicted mass (after rescaling) and width are 2774 and 233 MeV respectively which are in good agreement with the measured properties of the $D_1^*(2760)^0$. We therefore identify the $D_1^*(2760)^0$ as the $1^3D_1(c\overline{q})$ state.

The final state in this mass region is the unnatural parity $D_J(2750)^0$ state. For the purposes of this discussion we average the *BABAR* [2] and LHCb [11] measurements to obtain $M = 2744.7$ MeV and $\Gamma = 72.1$ MeV. The measured mass is marginally inconsistent with the predicted masses of the two $J = 2$ D-wave states; $M(1D_2) = 2782$ MeV and

TABLE XXIII. Partial widths and branching ratios for strong decays for the 2^3G_3 and $2G_4$ charm mesons. See the caption for Table IV for further explanations.

Initial state	Final state	Width (MeV)	BR (%)
$D(2^3G_3)$ 3721	$D\pi$	3.66	1.61
	$D\rho$	2.03	0.895
	$D^*\pi$	2.98	1.31
	$D^*\rho$	2.14	0.943
	$D(2^1S_0)\rho$	3.40	1.50
	$D(2^3S_1)\rho$	8.66	3.82
	$D(3^1S_0)\pi$	2.87	1.26
	$D(1P_1)\pi$	7.46	3.29
	$D(1P_1)\rho$	2.99	1.32
	$D(1P_1')\rho$	3.33	1.47
	$D(1^3P_2)\rho$	7.79	3.43
	$D(2P_1)\pi$	5.00	2.20
	$D(2^3P_2)\pi$	5.63	2.48
	$D(3P_1)\pi$	3.29	1.45
	$D(1D_2)\pi$	12.7	5.60
	$D(1D_2)\rho$	9.12	4.02
	$D(1^3D_3)\pi$	5.64	2.49
	$D(2D_2)\pi$	11.9	5.24
	$D(1F_3)\pi$	19.0	8.37
	$D(1^3F_4)\pi$	3.04	1.34
	$D(2F_3)\pi$	11.2	4.94
	$D(1G_4)\pi$	19.7	8.68
	$D_s(2P_1)K$	6.52	2.87
	$D_s(1F_3)K$	12.9	5.69
	Total	226.9	100
$D(2G_4)$ 3686	$D\rho$	4.85	3.72
	$D\omega$	1.60	1.23
	$D^*\rho$	3.16	2.42
	$D^*\omega$	1.04	0.797
	$D(2^1S_0)\rho$	7.33	5.62
	$D(2^1S_0)\omega$	2.45	1.88
	$D(2^3S_1)\pi$	12.4	9.50
	$D(2^3S_1)\rho$	8.01	6.14
	$D(2^3S_1)\omega$	2.58	1.98
	$D(1P_1)\rho$	3.32	2.54
	$D(1P_1')\rho$	2.72	2.08
	$D(1^3P_2)\pi$	9.39	7.19
	$D(1^3P_2)\rho$	4.96	3.80
	$D(1^3P_2)\omega$	1.60	1.23
	$D(2^3P_0)\pi$	1.99	1.52
	$D(2P_1)\pi$	2.70	2.07
	$D(2^3P_2)\pi$	4.61	3.53
	$D(1D_2)\pi$	2.22	1.70
	$D(1D_2)\rho$	17.4	13.3
	$D(1D_2)\omega$	5.81	4.45
	$D(1^3D_3)\pi$	3.71	2.84
	$D(1^3D_3)\rho$	2.27	1.74
	$D(1F_3)\pi$	1.64	1.26
	Total	130.5	100

TABLE XXIV. Partial widths and branching ratios for strong decays for the $2G_4'$ and 2^3G_5 charm mesons. See the caption for Table IV for further explanations.

Initial state	Final state	Width (MeV)	BR (%)
$D(2G_4')$ 3722	$D^*\pi$	7.51	3.16
	$D^*\rho$	3.49	1.47
	$D(2^1S_0)\rho$	4.08	1.72
	$D(2^3S_1)\rho$	9.51	4.00
	$D(3^3S_1)\pi$	5.08	2.14
	$D(1P_1)\rho$	3.52	1.48
	$D(1P_1')\rho$	3.06	1.29
	$D(1^3P_2)\pi$	10.8	4.55
	$D(1^3P_2)\rho$	7.31	3.08
	$D(2P_1)\pi$	3.04	1.28
	$D(2^3P_2)\pi$	7.56	3.18
	$D(2^3P_2)\eta$	3.40	1.43
	$D(3^3P_2)\pi$	3.43	1.44
	$D(1^3D_3)\pi$	16.3	6.86
	$D(1^3D_3)\rho$	11.6	4.88
	$D(1^3D_3)\omega$	3.91	1.65
	$D(2^3D_3)\pi$	13.5	5.68
	$D(1^3F_4)\pi$	21.8	9.18
	$D(2^3F_4)\pi$	11.7	4.93
	$D(1^3G_5)\pi$	21.3	8.97
	$D_s(2^3P_2)K$	6.93	2.92
	$D_s(1^3D_3)K$	3.75	1.58
	$D_s(1^3F_4)K$	13.7	5.77
	Total	237.6	100
$D(2^3G_5)$ 3685	$D\pi$	1.63	1.27
	$D^*\pi$	0.685	0.532
	$D^*\rho$	8.08	6.27
	$D^*\omega$	2.64	2.05
	$D(2^1S_0)\pi$	4.71	3.66
	$D(2^1S_0)\rho$	1.40	1.09
	$D(2^3S_1)\pi$	6.14	4.77
	$D(2^3S_1)\rho$	13.9	10.8
	$D(2^3S_1)\omega$	4.54	3.52
	$D(1P_1)\pi$	3.26	2.53
	$D(1P_1)\rho$	1.64	1.27
	$D(1P_1')\rho$	2.09	1.62
	$D(1^3P_2)\pi$	2.68	2.08
	$D(1^3P_2)\rho$	5.23	4.06
	$D(2P_1)\pi$	3.36	2.61
	$D(2P_1')\pi$	2.99	2.32
	$D(2^3P_2)\pi$	5.08	3.94
	$D(1D_2)\pi$	1.88	1.46
	$D(1D_2')\pi$	1.78	1.38
	$D(1^3D_3)\pi$	3.76	2.92
	$D(1^3D_3)\rho$	22.2	17.2
	$D(1^3D_3)\omega$	7.22	5.60
	$D(1^3F_4)\pi$	2.07	1.61
	$D_s(1^3P_2)K^*$	2.34	1.82
	Total	128.8	100

TABLE XXV. Partial widths and branching ratios for electromagnetic and strong decays for the $1S$, $2S$ and $3S$ charm-strange mesons. See the caption for Table IV for further explanations.

Initial state	Final state	Width (MeV)	BR (%)
D_s^* 2129	$D_s\gamma$	0.00103	100
	No Strong Decays		
	Total	0.00103	100
$D_s(2^3S_1)$ 2732	DK	40.1	32.5
	D^*K	72.3	58.6
	$D_s\eta$	7.35	5.96
	$D_s^*\eta$	3.65	2.96
	Total	123.4	100
$D_s(2^1S_0)$ 2673	D^*K	73.6	100
	Total	73.6	100
$D_s(3^3S_1)$ 3193	DK	7.71	6.28
	DK^*	3.52	2.87
	D^*K	12.8	10.4
	D^*K^*	4.89	3.98
	$D(2^1S_0)K$	13.8	11.2
	$D(2^3S_1)K$	14.3	11.6
	$D(1P_1)K$	24.8	20.2
	$D(1P_1')K$	0.642	0.523
	$D(1^3P_2)K$	26.3	21.4
	$D_s\eta$	0.269	0.219
	$D_s\eta'$	0.245	0.199
	$D_s\phi$	1.59	1.29
	$D_s^*\eta'$	1.85	1.51
	$D_s^*\phi$	6.51	5.30
	$D_s(1P_1)\eta$	0.949	0.773
	$D_s(1P_1')\eta$	2.39	1.95
	$D_s(1^3P_2)\eta$	0.337	0.274
	Total	122.8	100
$D_s(3^1S_0)$ 3154	DK^*	1.21	1.53
	D^*K	11.9	15.0
	D^*K^*	17.2	21.7
	$D(2^3S_1)K$	3.81	4.81
	$D(1^3P_2)K$	36.5	46.1
	$D_s\phi$	3.85	4.86
	$D_s^*\eta$	0.335	0.423
	$D_s^*\eta'$	2.37	2.99
	$D_s^*\phi$	0.357	0.451
	$D_s(1^3P_0)\eta$	1.63	2.06
	Total	79.2	100

TABLE XXVI. Partial widths and branching ratios for strong decays for the 4^3S_1 and 4^1S_0 charm-strange mesons. See the caption for Table IV for further explanations.

Initial state	Final state	Width (MeV)	BR (%)
$D_s(4^3S_1)$ 3575	DK	2.63	1.53
	DK^*	3.2	1.87
	D^*K	5.71	3.33
	D^*K^*	2.27	1.32
	$D(2^1S_0)K$	4.06	2.37
	$D(2^1S_0)K^*$	8.47	4.94
	$D(2^3S_1)K$	6.45	3.76
	$D(2^3S_1)K^*$	32.4	18.9
	$D(1P_1)K$	4.47	2.61
	$D(1P_1)K^*$	3.14	1.83
	$D(1P_1')K^*$	2.92	1.70
	$D(1^3P_2)K$	4.4	2.57
	$D(1^3P_2)K^*$	20.5	12.0
	$D(2P_1)K$	20.2	11.8
	$D(2^3P_2)K$	17.1	9.97
	$D(1D_2)K$	12.8	7.46
	$D(1^3D_3)K$	12.8	7.46
	$D_s^*\phi$	0.502	0.293
	Total	171.5	100
$D_s(4^1S_0)$ 3547	DK^*	3.16	2.37
	D^*K	6.48	4.87
	$D(2^1S_0)K^*$	17.5	13.2
	$D(2^3S_1)K$	6.32	4.75
	$D(2^3S_1)K^*$	6.5	4.88
	$D(1P_1)K^*$	9.47	7.12
	$D(1P_1')K^*$	3.85	2.89
	$D(1^3P_2)K$	4.68	3.52
	$D(1^3P_2)K^*$	20.9	15.7
	$D(2^3P_2)K$	22.6	17.0
	$D(1^3D_3)K$	24.4	18.3
	Total	133.1	100

$M(1D_2') = 2811$ MeV (after rescaling). The predicted widths are $\Gamma(1D_2) = 105$ MeV and $\Gamma(1D_2') = 244$ MeV respectively. Considering both the experimental uncertainty, which at least for the LHCb measurement is large, and the theoretical uncertainty, it is reasonable to identify the $D_J(2750)^0$ with the $1D_2(c\overline{q})$ state. This identification can be verified by observing the $D_J(2750)^0$ in other decay modes. For example, $\mathrm{BR}(1D_2 \to D\rho) = 58\%$ while $\mathrm{BR}(1D_2' \to D\rho) = 2.4\%$. This should be a relatively simple final state to observe. The second largest decay mode for the $1D_2'$ is $\mathrm{BR}(1D_2' \to D^*\pi) \sim 38\%$ vs $\mathrm{BR}(1D_2 \to D^*\pi) \sim 20\%$. Finally, the next largest BR for $1D_2'$ is $\mathrm{BR}(1D_2' \to D(1^3P_2)\pi) = 37\%$ vs $\mathrm{BR}(1D_2 \to D(1^3P_2)\pi) < 1\%$, which is another discriminator between these two possibilities although this final state is likely to be difficult to observe.

We conclude that the $D_1^*(2760)^0$, $D_3^*(2760)^0$ and $D_J(2750)^0$ states can be identified with the $1^3D_1(c\overline{q})$, $1^3D_3(c\overline{q})$ and $1D_2(c\overline{q})$ quark model states, respectively. Our identification of the $D_J(2750)^0$ with the $1D_2(c\overline{q})$ is consistent with other studies [17,20,25,91,98] although in some cases they label this state with the prime.

With three of the four $1D$ states observed by the *BABAR* and LHCb collaborations there is one remaining $1D$ state to be found. However, with four overlapping states it is not an easy task to disentangle them based solely on mass and total width measurements and to make precise measurements of their properties. Measuring BRs will be useful for

TABLE XXVII. Partial widths and branching ratios for strong decays for the 5^3S_1 and 5^1S_0 charm-strange mesons. See the caption for Table IV for further explanations.

Initial state	Final state	Width (MeV)	BR (%)
$D_s(5^3S_1)$ 3912	DK	1.10	0.642
	DK^*	1.95	1.14
	D^*K	2.94	1.72
	D^*K^*	3.73	2.18
	$D(2^1S_0)K$	1.60	0.933
	$D(2^3S_1)K$	3.19	1.86
	$D(3^1S_0)K$	2.31	1.35
	$D(3^3S_1)K$	3.08	1.80
	$D(1P_1)K$	1.85	1.08
	$D(1^3P_2)K$	2.13	1.24
	$D(2P_1)K$	5.44	3.17
	$D(2P_1)K^*$	13.6	7.93
	$D(2^3P_2)K$	5.03	2.93
	$D(2^3P_2)K^*$	24.6	14.4
	$D(3P_1)K$	10.6	6.18
	$D(3P_1')K$	3.07	1.79
	$D(3^3P_2)K$	6.67	3.89
	$D(1D_2)K$	2.30	1.34
	$D(1D_2)K^*$	3.97	2.32
	$D(1^3D_3)K$	2.16	1.26
	$D(1^3D_3)K^*$	12.4	7.23
	$D(2D_2)K$	17.5	10.2
	$D(2^3D_3)K$	15.0	8.75
	$D(1F_3)K$	6.82	3.98
	$D(1^3F_4)K$	6.60	3.85
	Total	171.4	100
$D_s(5^1S_0)$ 3894	DK^*	2.06	1.23
	D^*K	3.34	1.99
	$D(2^3S_1)K$	3.62	2.16
	$D(2^3S_1)K^*$	4.13	2.47
	$D(3^3S_1)K$	2.42	1.45
	$D(1^3P_2)K$	2.35	1.40
	$D(1^3P_2)K^*$	2.05	1.22
	$D(2P_1)K^*$	21.9	13.1
	$D(2P_1')K^*$	10.0	5.97
	$D(2^3P_2)K$	6.28	3.75
	$D(2^3P_2)K^*$	12.2	7.29
	$D(3^3P_0)K$	2.90	1.73
	$D(3^3P_2)K$	6.45	3.85
	$D(1D_2)K^*$	9.88	5.90
	$D(1^3D_3)K$	2.45	1.46
	$D(1^3D_3)K^*$	12.4	7.41
	$D(2^3D_3)K$	30.7	18.3
	$D(1^3F_4)K$	16.9	10.1
	Total	167.4	100

solidifying the spectroscopic assignments given above and resolving ambiguities and inconsistencies. For example, the LHCb collaboration resolved the $D_J^*(2760)$ into $J=1$ and $J=3$ states. Our calculations predict $\Gamma(D\pi)/\Gamma(D^*\pi) =$ 1.8 for the $1^3D_1(c\bar{q})$ and 1.3 for $1^3D_3(c\bar{q})$. These are inconsistent with the *BABAR* measurement of $0.42 \pm 0.05 \pm 0.11$ for the $D_J^*(2760)^0$ [2]. It is possible that a new measurement will resolve this discrepancy but it is also possible that the $D^*\pi$ signal contains significant contributions from broad overlapping D_2 states. Further useful information about these states can be obtained by measuring BRs into other final states such as to $D\rho$ and D_sK with the relevant BRs given in Table XIII.

TABLE XXVIII. Partial widths and branching ratios for strong and electromagnetic decays for the $1P$ charm-strange mesons. See the caption for Table IV for further explanations.

Initial state	Final state	Width (MeV)	BR (%)
$D_s(1^3P_0)$ 2484	$D_s^*\gamma$	0.00901	0.00407
	DK	221	99.8
	Total	221	100
$D_s(1P_1)$ 2549	$D_s\gamma$	0.0152	11.2
	$D_s^*\gamma$	0.00540	3.99
	D^*K	0.129	95.3
	Total	0.135	100
$D_s(1P_1')$ 2556	$D_s\gamma$	0.00923	0.00659
	$D_s^*\gamma$	0.00961	0.00687
	D^*K	140.	100
	Total	140.	100
$D_s(1^3P_2)$ 2592	$D_s^*\gamma$	0.0189	0.188
	DK	9.40	93.4
	D^*K	0.545	5.41
	$D_s\eta$	0.105	1.04
	Total	10.07	100

C. The $D_J(3000)^0$ and $D_J^*(3000)^0$ states

LHCb has reported two states around 3000 MeV, the natural parity state $D_J^*(3000)^0$ with mass $= 3008.1 \pm 4.0$ MeV and width $= 110.5 \pm 11.5$ MeV and the unnatural parity state $D_J(3000)^0$ with mass $= 2971.8 \pm 8.7$ MeV and width $= 188.1 \pm 44.8$ MeV [11]. Our calculations expect the $2P$, $3S$ and $1F$ multiplets to lie in this mass region consisting of the natural parity 2^3P_2, 2^3P_0, 3^3S_1, 1^3F_4 and 1^3F_2 states and the unnatural parity $2P_1'$, $2P_1$, 3^1S_0, $1F_3'$ and $1F_3$ states. All of these states are expected to have widths in the range of 114 to 270 MeV which, given the theoretical and experimental uncertainties, cannot by themselves be used to rule out any of the possibilities. To help us narrow the possibilities we summarize the predicted properties of the $2P$, $3S$, and $1F$ multiplets in Table XLV. We list BRs for the simpler final states under the assumption that they will be easiest to observe. We also include some final states with larger BRs as they contribute to the total width but expect that in many cases they will be challenging to reconstruct.

TABLE XXIX. Partial widths and branching ratios for strong decays for the $2P$ charm-strange mesons. See the caption for Table IV for further explanations.

Initial state	Final state	Width (MeV)	BR (%)
$D_s(2^3P_0)$ 3005	DK	50.9	35.0
	D^*K^*	39.3	27.0
	$D(1P_1)K$	41.9	28.8
	$D_s\eta$	0.602	0.414
	$D_s\eta'$	12.9	8.86
	Total	145.6	100
$D_s(2P_1)$ 3018	DK^*	6.54	4.57
	D^*K	61.3	42.9
	D^*K^*	38.9	27.2
	$D(1^3P_0)K$	4.95	3.46
	$D(1P_1)K$	3.52	2.46
	$D(1P_1')K$	1.29	0.902
	$D(1^3P_2)K$	0.670	0.469
	$D_s\phi$	16.2	11.3
	$D_s^*\eta$	9.65	6.75
	Total	143.0	100
$D_s(2P_1')$ 3038	DK^*	32.1	21.7
	D^*K	36.5	24.7
	D^*K^*	29.7	20.1
	$D(1^3P_0)K$	1.14	0.772
	$D(1P_1)K$	12.2	8.26
	$D(1P_1')K$	3.38	2.29
	$D(1^3P_2)K$	28.4	19.2
	$D_s\phi$	4.15	2.81
	$D_s^*\eta$	0.153	0.104
	Total	147.6	100
$D_s(2^3P_2)$ 3048	DK	8.54	6.49
	DK^*	20.7	15.7
	D^*K	30.8	23.4
	D^*K^*	48.9	37.2
	$D(1P_1)K$	2.45	1.86
	$D(1P_1')K$	4.88	3.71
	$D(1^3P_2)K$	5.17	3.93
	$D_s\eta$	3.38	2.57
	$D_s\eta'$	0.504	0.383
	$D_s\phi$	0.275	0.209
	$D_s^*\eta$	5.90	4.49
	Total	131.5	100

TABLE XXX. Partial widths and branching ratios for strong decays for the 3^3P_0 and $3P_1$ charm-strange mesons. See the caption for Table IV for further explanations.

Initial state	Final state	Width (MeV)	BR (%)
$D_s(3^3P_0)$ 3412	DK	20.3	19.5
	D^*K^*	2.90	2.79
	$D(2^1S_0)K$	15.7	15.1
	$D(1^3P_0)K^*$	4.20	4.04
	$D(1P_1)K$	10.1	9.72
	$D(1P_1)K^*$	9.76	9.39
	$D(1P_1')K^*$	11.6	11.2
	$D(1^3P_2)K^*$	0.968	0.931
	$D(1D_2)K$	20.8	20.0
	$D(1D_2')K$	0.282	0.271
	$D_s^*\phi$	4.03	3.88
	$D_s(1P_1)\eta$	2.01	1.93
	Total	103.9	100
$D_s(3P_1)$ 3416	DK^*	6.90	4.62
	D^*K	13.0	8.71
	D^*K^*	2.53	1.70
	$D(2^3S_1)K$	29.7	19.9
	$D(1^3P_0)K$	2.13	1.43
	$D(1P_1)K$	0.558	0.374
	$D(1P_1)K^*$	28.8	19.3
	$D(1P_1')K$	0.396	0.265
	$D(1P_1')K^*$	11.6	7.77
	$D(1^3P_2)K$	33.5	22.4
	$D(1^3P_2)K^*$	3.89	2.61
	$D(1^3D_1)K$	1.76	1.18
	$D(1D_2)K$	1.76	1.18
	$D(1^3D_3)K$	1.90	1.27
	$D_s^*\phi$	2.03	1.36
	$D_s(2^3S_1)\eta$	3.25	2.18
	$D_s(1^3P_2)\eta$	3.44	2.31
	Total	149.2	100

Before proceeding we note that LHCb comments that the resonance parameters are strongly correlated to the background parametrization and the fit does not include the broad $D_0^*(2420)$ [11]. Thus, one should be cautious in how literally one takes the LHCb values.

Given the general uncertainties of our predictions it is difficult to make definitive spectroscopic assignments for the $D_J^*(3000)$ and $D_J(3000)$ states. At best we can narrow down the possibilities, present our most likely assignment and suggest future measurements that could uniquely identify these states. With this caveat we note that in general our mass predictions tend to overestimate masses of excited states rather than underestimate them. The $2P$ multiplet lies around 2900 MeV, 100 MeV below the observed masses so we consider it less likely that the $D_J^*(3000)$ and $D_J(3000)$ are $2P$ states.

For the natural parity states, this leaves the 3^3S_1, 1^3F_4 and 1^3F_2. We calculate a total width for the 1^3F_2 of 243 MeV versus the measured width of 110.5 ± 11.5 MeV. As we have stated previously, we would not be surprised if our width predictions are off by a factor of two. Nevertheless it is likely that the properties of the 1^3F_2 are inconsistent with those of the $D_J^*(3000)$. As a final discriminator we consider signal strengths assuming that the state with the largest expected signal strength is the state most likely to first be observed. Signal strengths are a product of the production cross section and final state BR. We surmise that the cross section for orbitally excited states

TABLE XXXI. Partial widths and branching ratios for strong decays for the $3P_1'$ and 3^3P_2 charm-strange mesons. See the caption for Table IV for further explanations.

Initial state	Final state	Width (MeV)	BR (%)
$D_s(3P_1')$	DK^*	7.44	6.06
3433	D^*K	16.4	13.4
	D^*K^*	4.61	3.76
	$D(2^3S_1)K$	12.0	9.78
	$D(1^3P_0)K^*$	2.27	1.85
	$D(1P_1)K$	2.24	1.83
	$D(1P_1)K^*$	9.77	7.96
	$D(1P_1')K$	1.49	1.21
	$D(1P_1')K^*$	10.1	8.23
	$D(1^3P_2)K$	7.84	6.39
	$D(1^3P_2)K^*$	10.5	8.56
	$D(2P_1)K$	1.48	1.21
	$D(1D_2)K$	7.62	6.21
	$D(1^3D_3)K$	20.2	16.5
	$D_s^*\phi$	1.99	1.62
	$D_s(2^3S_1)\eta$	1.79	1.46
	$D_s(1^3P_2)\eta$	2.57	2.09
	Total	122.7	100
$D_s(3^3P_2)$	DK	2.25	1.63
3439	DK^*	4.36	3.15
	D^*K	7.53	5.44
	D^*K^*	5.37	3.88
	$D(2^1S_0)K$	7.53	5.44
	$D(2^3S_1)K$	16.2	11.7
	$D(1^3P_0)K^*$	2.02	1.46
	$D(1P_1)K$	10.4	7.51
	$D(1P_1)K^*$	4.49	3.24
	$D(1P_1')K$	2.34	1.69
	$D(1P_1')K^*$	9.17	6.62
	$D(1^3P_2)K$	12.9	9.32
	$D(1^3P_2)K^*$	35.4	25.6
	$D(1D_2)K$	1.33	0.961
	$D(1D_2')K$	2.03	1.47
	$D(1^3D_3)K$	3.97	2.87
	$D_s^*\phi$	1.72	1.24
	$D_s(2^1S_0)\eta$	2.21	1.60
	$D_s(2^3S_1)\eta$	2.47	1.78
	$D_s(1P_1)\eta$	1.79	1.29
	$D_s(1^3P_2)\eta$	1.62	1.17
	Total	138.4	100

TABLE XXXII. Partial widths and branching ratios for strong decays for the 4^3P_0 and $4P_1$ charm-strange mesons. See the caption for Table IV for further explanations.

Initial state	Final state	Width (MeV)	BR (%)
$D_s(4^3P_0)$	DK	10.2	9.76
3764	D^*K^*	5.10	4.88
	$D(2^1S_0)K$	7.88	7.54
	$D(2^3S_1)K^*$	6.97	6.67
	$D(3^1S_0)K$	5.19	4.97
	$D(1P_1)K$	6.66	6.37
	$D(1^3P_2)K^*$	0.942	0.901
	$D(2P_1)K$	10.9	10.4
	$D(1^3D_1)K^*$	1.21	1.16
	$D(1D_2)K$	2.91	2.78
	$D(1D_2)K^*$	3.76	3.60
	$D(2D_2)K$	13.1	12.5
	$D(1F_3)K$	12.7	12.1
	$D_s(2^3S_1)\phi$	1.59	1.52
	$D_s(3^1S_0)\eta$	4.27	4.08
	$D_s(1^3P_2)\phi$	2.00	1.91
	$D_s(2P_1)\eta$	3.62	3.46
	$D_s(1D_2)\eta$	1.78	1.70
	Total	104.5	100
$D_s(4P_1)$	DK^*	5.35	4.04
3764	D^*K	5.01	3.78
	D^*K^*	3.79	2.86
	$D(2^3S_1)K$	8.03	6.06
	$D(2^3S_1)K^*$	4.91	3.70
	$D(3^3S_1)K$	16.3	12.3
	$D(1^3P_0)K$	1.79	1.35
	$D(1^3P_2)K$	7.34	5.54
	$D(2^3P_2)K$	28.6	21.6
	$D(1D_2)K^*$	6.81	5.14
	$D(1D_2')K^*$	1.40	1.06
	$D(1^3D_3)K$	15.4	11.6
	$D(2^3D_1)K$	2.79	2.10
	$D(1^3F_4)K$	2.22	1.67
	$D_s(2^3S_1)\phi$	2.28	1.72
	$D_s(2^3P_2)\eta$	2.85	2.15
	$D_s(1^3D_3)\eta$	1.68	1.27
	Total	132.6	100

is suppressed compared to states with small orbital angular momentum but we do not know how to accurately calculate the production cross section for charm mesons so only consider the final state BR. The BRs for the two remaining possibilities are $\mathrm{BR}(D_1^*(3^3S_1) \to D\pi) \simeq 3\%$ vs $\mathrm{BR}(D_4^*(1^3F_4) \to D\pi) \simeq 12\%$. On this basis we tentatively identify the $D_J^*(3000)$ as the $D_4^*(1^3F_4)$ state but note that this conclusion is based on a number of unsubstantiated assumptions.

The key to confirming this identification will be measuring BRs to other final states and ratios of BRs. Observing the $D_J^*(3000)$ in the $D^*\pi$ final state would rule out the 2^3P_0. Measuring the ratio $R = \mathrm{BR}(D^*\pi)/\mathrm{BR}(D\pi)$ could narrow down the options. Large ratios would imply the 2^3P_2 with $R \sim 3.4$ or 3^3S_1 with $R \sim 1.7$ while a small ratio would imply 1^3F_2 with $R \sim 0.8$ and a ratio ~ 1 would imply the 1^3F_4. Undoubtedly the experimental errors will be large to start with and therefore not precise enough, along with the theoretical uncertainties, to narrow down the possibilities to one specific state. For example, the 1^3F_4 decays almost half the time to $D^*\rho$ while the 3^3S_1 and 1^3F_2 have much smaller

TABLE XXXIII. Partial widths and branching ratios for strong decays for the $4P_1'$ and 4^3P_2 charm-strange mesons. See the caption for Table IV for further explanations.

Initial state	Final state	Width (MeV)	BR (%)
$D_s(4P_1')$ 3778	DK^*	3.89	3.34
	D^*K	9.34	8.02
	D^*K^*	4.48	3.85
	$D(2^3S_1)K$	7.24	6.22
	$D(2^3S_1)K^*$	2.13	1.83
	$D(3^3S_1)K$	2.95	2.53
	$D(1P_1')K$	1.54	1.32
	$D(1^3P_2)K$	5.05	4.34
	$D(2P_1)K$	2.40	2.06
	$D(2^3P_2)K$	7.70	6.61
	$D(1D_2)K$	1.25	1.07
	$D(1D_2)K^*$	2.70	2.32
	$D(1D_2')K^*$	2.48	2.13
	$D(1^3D_3)K$	3.25	2.79
	$D(1^3D_3)K^*$	3.51	3.01
	$D(2D_2)K$	5.55	4.77
	$D(2^3D_3)K$	10.4	8.93
	$D(1F_3)K$	4.58	3.93
	$D(1^3F_4)K$	12.4	10.6
	$D_s(3^3S_1)\eta$	6.27	5.38
	$D_s(2^3P_2)\eta$	3.62	3.11
	$D_s(1^3D_3)\eta$	1.59	1.37
	Total	116.5	100
$D_s(4^3P_2)$ 3783	DK^*	1.73	1.39
	D^*K	2.76	2.22
	D^*K^*	7.41	5.97
	$D(2^1S_0)K$	2.09	1.68
	$D(2^3S_1)K$	4.50	3.63
	$D(2^3S_1)K^*$	4.10	3.31
	$D(3^1S_0)K$	5.90	4.76
	$D(3^3S_1)K$	10.2	8.22
	$D(1P_1)K$	2.60	2.10
	$D(1P_1')K$	1.98	1.60
	$D(1^3P_2)K$	3.53	2.85
	$D(1^3P_2)K^*$	2.13	1.72
	$D(2P_1)K$	10.8	8.71
	$D(2P_1')K$	1.26	1.02
	$D(2^3P_2)K$	11.1	8.95
	$D(1D_2)K$	5.36	4.32
	$D(1D_2)K^*$	1.68	1.35
	$D(1D_2')K^*$	1.57	1.27
	$D(1^3D_3)K$	4.94	3.98
	$D(1^3D_3)K^*$	10.6	8.55
	$D(2D_2')K$	2.87	2.31
	$D(2^3D_3)K$	2.20	1.77
	$D(1^3F_4)K$	2.66	2.14
	$D_s(2^3S_1)\phi$	3.78	3.05
	$D_s(2P_1)\eta$	2.03	1.64
	$D_s(2^3P_2)\eta$	1.57	1.27
	Total	124.0	100

TABLE XXXIV. Partial widths and branching ratios for strong decays for the $1D$ charm-strange mesons. See the caption for Table IV for further explanations.

Initial state	Final state	Width (MeV)	BR (%)
$D_s(1^3D_1)$ 2899	DK	93.2	47.3
	DK^*	29.5	15.0
	D^*K	50.2	25.5
	$D_s\eta$	17.5	8.88
	$D_s^*\eta$	6.62	3.36
	Total	197.2	100
$D_s(1D_2)$ 2900	DK^*	93.2	81.0
	D^*K	21.1	18.3
	$D_s^*\eta$	0.698	0.606
	Total	115.1	100
$D_s(1D_2')$ 2926	DK^*	7.92	4.05
	D^*K	163	83.4
	$D_s^*\eta$	24.6	12.6
	Total	195	100
$D_s(1^3D_3)$ 2917	DK	26.5	57.7
	DK^*	1.52	3.31
	D^*K	15.7	34.2
	$D_s\eta$	1.59	3.46
	$D_s^*\eta$	0.573	1.25
	Total	46.0	100

BRs to this final state. Finally, the 1^3F_2 has a much larger BR to $D\rho$ than does the 3^3S_1. Thus, observing more final states can either confirm the hypothesis that the $D_J^*(3000)$ is the $D_4^*(1^3F_4)$ or direct us to an alternative identification.

We follow the same approach when trying to identify the unnatural parity $D_J(3000)$ state. We set aside the $2P_1$ and $2P_1'$ as they are likely to be too low in mass. None of the three remaining states can be ruled out based on their total widths, considering both the experimental and theoretical uncertainties. The 3^1S_0 mass is closest to the measured mass while the $1F_3$ and $1F_3'$ have much larger BRs to the observed $D^*\pi$ final state. We slightly favor the $D(3^1S_0)$ identification but more information is needed to make a more informed identification. For example, if the $D_J(3000)$ were observed in the $D\rho$ final state the 3^1S_0 would be ruled out. Measuring the ratios of BRs of $R = \mathrm{BR}(D\rho)/\mathrm{BR}(D^*\pi)$ would provide a powerful discriminator between the remaining options: $2P_1$, $2P_1'$, $1F_3$ and $1F_3'$. Numerous other final states could be used to help identify the quark model assignment of the $D_J(3000)$ but are typically more difficult to reconstruct so are unlikely to provide useful input in the near future.

We therefore tentatively identify the $D_J^*(3000)$ as the $D_4^*(1^3F_4)$ state and favor the $D_J(3000)$ as the $D(3^1S_0)$ state although we do not rule out the $1F_3$ and $1F_3'$ assignments. Previous studies have come to the same conclusions [91]. However, Ref. [17] agrees with our

TABLE XXXV. Partial widths and branching ratios for strong decays for the $2D$ charm-strange mesons. See the caption for Table IV for further explanations.

Initial state	Final state	Width (MeV)	BR (%)
$D_s(2^3D_1)$ 3306	DK	29.5	13.9
	DK^*	6.13	2.89
	D^*K	12.2	5.76
	D^*K^*	53.1	25.1
	$D(2^1S_0)K$	21.8	10.3
	$D(2^3S_1)K$	11.8	5.57
	$D(1P_1)K$	34.8	16.4
	$D(1P_1')K$	3.28	1.55
	$D(1^3P_2)K$	21.9	10.3
	$D_s^*\phi$	3.95	1.87
	$D_s(2^1S_0)\eta$	3.74	1.77
	$D_s(1P_1)\eta$	3.94	1.86
	Total	211.8	100
$D_s(2D_2)$ 3298	DK^*	21.1	19.8
	D^*K	12.1	11.4
	D^*K^*	26.1	24.5
	$D(2^3S_1)K$	4.09	3.84
	$D(1^3P_0)K$	6.02	5.66
	$D(1P_1)K$	5.68	5.34
	$D(1P_1')K$	5.47	5.14
	$D(1^3P_2)K$	13.1	12.3
	$D_s^*\eta$	4.02	3.78
	$D_s^*\phi$	4.30	4.04
	Total	106.4	100
$D_s(2D_2')$ 3323	DK^*	10.6	5.22
	D^*K	43.5	21.4
	D^*K^*	31.4	15.5
	$D(2^3S_1)K$	37.3	18.4
	$D(1^3P_0)K$	2.63	1.30
	$D(1P_1)K$	8.06	3.97
	$D(1P_1')K$	6.52	3.21
	$D(1^3P_2)K$	42.4	20.9
	$D_s^*\phi$	4.33	2.13
	$D_s(2^3S_1)\eta$	2.79	1.37
	$D_s(1^3P_2)\eta$	5.91	2.91
	Total	203.0	100
$D_s(2^3D_3)$ 3311	DK^*	3.95	4.49
	D^*K	3.86	4.39
	D^*K^*	22.2	25.3
	$D(2^1S_0)K$	5.45	6.20
	$D(2^3S_1)K$	3.19	3.63
	$D(1P_1)K$	10.4	11.8
	$D(1P_1')K$	9.39	10.7
	$D(1^3P_2)K$	15.2	17.3
	$D_s^*\eta$	1.84	2.09
	$D_s^*\phi$	6.64	7.55
	$D_s(1P_1')\eta$	1.43	1.63
	$D_s(1^3P_2)\eta$	1.21	1.38
	Total	87.9	100

TABLE XXXVI. Partial widths and branching ratios for strong decays for the 3^3D_1 and $3D_2$ charm-strange mesons. See the caption for Table IV for further explanations.

Initial state	Final state	Width (MeV)	BR (%)
$D_s(3^3D_1)$ 3658	DK	12.8	6.45
	DK^*	3.76	1.89
	D^*K	5.56	2.80
	D^*K^*	11.1	5.59
	$D(2^1S_0)K$	8.73	4.40
	$D(2^3S_1)K$	4.48	2.26
	$D(2^3S_1)K^*$	18.1	9.12
	$D(3^1S_0)K$	10.7	5.39
	$D(3^3S_1)K$	3.69	1.86
	$D(1P_1)K$	11.9	6.00
	$D(1^3P_2)K$	4.32	2.18
	$D(1^3P_2)K^*$	21.1	10.6
	$D(2P_1)K$	21.7	10.9
	$D(2P_1')K$	2.61	1.32
	$D(2^3P_2)K$	12.6	6.35
	$D(1D_2)K$	8.40	4.23
	$D(1^3D_3)K$	9.37	4.72
	$D(1F_3)K$	5.38	2.71
	$D_s(2P_1)\eta$	5.45	2.75
	$D_s(1D_2)\eta$	3.81	1.92
	Total	198.5	100
$D_s(3D_2)$ 3650	DK^*	12.1	10.0
	D^*K	3.92	3.25
	D^*K^*	8.52	7.05
	$D(2^1S_0)K^*$	2.05	1.70
	$D(2^3S_1)K$	7.02	5.81
	$D(2^3S_1)K^*$	14.5	12.0
	$D(1^3P_0)K$	2.65	2.19
	$D(1P_1)K^*$	2.57	2.13
	$D(1P_1')K$	1.72	1.42
	$D(1^3P_2)K$	7.52	6.23
	$D(1^3P_2)K^*$	11.2	9.27
	$D(2^3P_0)K$	4.2	3.48
	$D(2P_1)K$	4.32	3.58
	$D(2P_1')K$	3.09	2.56
	$D(2^3P_2)K$	8.57	7.10
	$D(1D_2)K$	3.26	2.70
	$D(1^3D_3)K$	8.45	7.00
	$D_s(2^3S_1)\eta$	3.47	2.87
	$D_s(1^3P_2)\eta$	2.05	1.70
	Total	120.8	100

identification of the $D_J^*(3000)$ but suggests that the $D_J(3000)$ is a $2P_1$ state, Ref. [23] identifies the $D_J^*(3000)$ as either the $D_4^*(1^3F_4)$ or $D_2^*(1^3F_2)$ and the $D_J(3000)$ as either the $D_3(1F_3)$ or $D_1'(2P_1')$, and Ref. [21] argues that the $D_J(3000)$ and $D_J^*(3000)$ are the $2P_1$ and 2^3P_0 respectively. Still other assignments appear in the

TABLE XXXVII. Partial widths and branching ratios for strong decays for the $3D_2'$ and 3^3D_3 charm-strange mesons. See the caption for Table IV for further explanations.

Initial state	Final state	Width (MeV)	BR (%)
$D_s(3D_2')$ 3672	DK^*	2.88	1.38
	D^*K	19.3	9.27
	D^*K^*	9.72	4.67
	$D(2^1S_0)K^*$	11.6	5.57
	$D(2^3S_1)K$	13.9	6.67
	$D(2^3S_1)K^*$	15.3	7.34
	$D(3^3S_1)K$	14.1	6.77
	$D(1P_1)K^*$	8.24	3.96
	$D(1P_1')K$	2.82	1.35
	$D(1^3P_2)K$	14.1	6.77
	$D(1^3P_2)K^*$	11.4	5.47
	$D(2P_1)K$	5.97	2.87
	$D(2P_1')K$	3.63	1.74
	$D(2^3P_2)K$	24.0	11.5
	$D(1D_2)K$	5.17	2.48
	$D(1^3D_3)K$	12.4	5.95
	$D(1^3F_4)K$	7.85	3.77
	$D_s(2^3P_2)\eta$	7.14	3.43
	$D_s(1^3D_3)\eta$	4.11	1.97
	Total	208.3	100
$D_s(3^3D_3)$ 3661	DK^*	0.954	0.806
	D^*K	1.43	1.21
	D^*K^*	14.7	12.4
	$D(2^1S_0)K^*$	5.92	5.00
	$D(2^3S_1)K$	2.58	2.18
	$D(2^3S_1)K^*$	17.8	15.0
	$D(1P_1)K$	1.32	1.11
	$D(1P_1)K^*$	3.96	3.34
	$D(1P_1')K$	3.81	3.22
	$D(1^3P_2)K$	3.95	3.34
	$D(1^3P_2)K^*$	10.4	8.78
	$D(2P_1)K$	7.86	6.64
	$D(2P_1')K$	6.33	5.35
	$D(2^3P_2)K$	9.61	8.11
	$D(1D_2)K$	5.05	4.26
	$D(1^3D_3)K$	6.90	5.83
	$D_s(1^3P_2)\phi$	2.85	2.41
	Total	118.4	100

literature [20]. Clearly further measurements of other BRs are needed to settle the issue.

VI. CLASSIFICATION OF THE OBSERVED CHARM-STRANGE MESONS

We summarize the properties of the recently observed charm-strange mesons in Table XLVI.

TABLE XXXVIII. Partial widths and branching ratios for strong decays for the $1F$ charm-strange mesons. See the caption for Table IV for further explanations.

Initial state	Final state	Width (MeV)	BR (%)
$D_s(1^3F_2)$ 3208	DK	44.8	15.3
	DK^*	33.7	11.5
	D^*K	37.7	12.9
	D^*K^*	29.8	10.2
	$D(1P_1)K$	97.4	33.3
	$D(1P_1')K$	2.53	0.865
	$D(1^3P_2)K$	13.1	4.48
	$D_s\eta$	7.90	2.70
	$D_s\eta'$	3.65	1.25
	$D_s\phi$	3.28	1.12
	$D_s^*\eta$	5.33	1.82
	$D_s(1P_1)\eta$	9.68	3.31
	Total	292.5	100
$D_s(1F_3)$ 3186	DK^*	79.9	43.7
	D^*K	41.2	22.6
	D^*K^*	48.8	26.7
	$D_s\phi$	6.70	3.67
	$D_s^*\eta$	2.08	1.14
	Total	182.6	100
$D_s(1F_3')$ 3218	DK^*	20.2	6.26
	D^*K	93.2	28.9
	D^*K^*	55.9	17.3
	$D(1P_1)K$	2.49	0.772
	$D(1^3P_2)K$	123	38.1
	$D_s^*\eta$	14.1	4.37
	$D_s(1^3P_2)\eta$	8.72	2.70
	Total	323	100
$D_s(1^3F_4)$ 3190	DK	28.8	15.9
	DK^*	8.37	4.61
	D^*K	24.7	13.6
	D^*K^*	112	61.7
	Total	182	100

A. The $D_{s1}^*(2709)^\pm$, $D_{s1}^*(2860)^-$ and $D_{s3}^*(2860)^-$ states

The $D_{s1}^*(2709)^\pm$ [3–5,12] and $D_{sJ}^*(2860)^-$ [3,5,12] were first observed by the Belle [4], *BABAR* [3,5] and LHCb [12] collaborations. More recently the LHCb collaboration has measured the properties of the $D_{sJ}^*(2860)^-$ more precisely and found that it is comprised of two overlapping states, the $D_{s1}^*(2860)^-$ and $D_{s3}^*(2860)^-$ with $J^P = 1^-$ and 3^- respectively [13,14]. With this new information it was argued that the $D_{s1}^*(2709)^\pm$ is the $2^3S_1(c\bar{s})$ state and the $D_{s1}^*(2860)^-$ and $D_{s3}^*(2860)^-$ are the $1^3D_1(s\bar{c})$ and $1^3D_3(s\bar{c})$ states respectively [13–15,19,31]. The largest overall discrepancy between theory and experiment is for the ratio $\Gamma(2^3S_1 \to D^*K)/\Gamma(2^3S_1 \to DK)$. However, it was argued that this discrepancy could be explained by treating the $D_{s1}^*(2709)^\pm$ as a mixture of $2^3S_1(c\bar{s})$ and $1^3D_1(c\bar{s})$

TABLE XXXIX. Partial widths and branching ratios for strong decays for the 2^3F_2 and $2F_3$ charm-strange mesons. See the caption for Table IV for further explanations.

Initial state	Final state	Width (MeV)	BR (%)
$D_s(2^3F_2)$ 3562	DK	19.5	7.77
	DK^*	10.0	3.98
	D^*K	13.7	5.46
	D^*K^*	18.6	7.41
	$D(2^1S_0)K$	5.25	2.09
	$D(2^1S_0)K^*$	4.94	1.97
	$D(2^3S_1)K$	6.14	2.45
	$D(1^3P_0)K^*$	4.83	1.92
	$D(1P_1)K$	28.3	11.3
	$D(1P_1)K^*$	9.88	3.94
	$D(1P_1')K$	3.84	1.53
	$D(1P_1')K^*$	7.28	2.90
	$D(1^3P_2)K$	10.9	4.34
	$D(1^3P_2)K^*$	6.91	2.75
	$D(2P_1)K$	36.8	14.7
	$D(2P_1')K$	0.399	0.159
	$D(2^3P_2)K$	4.53	1.80
	$D(1D_2)K$	28.2	11.2
	$D(1^3D_3)K$	8.13	3.24
	$D_s^*\phi$	3.26	1.30
	$D_s(1D_2)\eta$	6.25	2.49
	Total	251.0	100
$D_s(2F_3)$ 3540	DK^*	24.9	17.7
	D^*K^*	16.4	11.6
	$D(2^1S_0)K^*$	7.15	5.07
	$D(2^3S_1)K$	18.5	13.1
	$D(1^3P_0)K$	2.41	1.71
	$D(1^3P_0)K^*$	1.69	1.20
	$D(1P_1)K$	1.38	0.979
	$D(1P_1)K^*$	13.0	9.22
	$D(1P_1')K$	2.98	2.11
	$D(1P_1')K^*$	5.54	3.93
	$D(1^3P_2)K$	21.0	14.9
	$D(1^3P_2)K^*$	9.18	6.51
	$D(1^3D_1)K$	2.48	1.76
	$D(1D_2)K$	3.95	2.80
	$D(1^3D_3)K$	1.67	1.18
	Total	141.0	100

TABLE XL. Partial widths and branching ratios for strong decays for the $2F_3'$ and 2^3F_4 charm-strange mesons. See the caption for Table IV for further explanations.

Initial state	Final state	Width (MeV)	BR (%)
$D_s(2F_3')$ 3569	DK^*	0.815	0.326
	D^*K	36.2	14.5
	D^*K^*	17.5	6.99
	$D(2^3S_1)K$	13.7	5.47
	$D(1P_1)K^*$	5.04	2.01
	$D(1P_1')K$	3.56	1.42
	$D(1P_1')K^*$	7.73	3.09
	$D(1^3P_2)K$	36.3	14.5
	$D(1^3P_2)K^*$	18.6	7.43
	$D(2^3P_2)K$	41.7	16.7
	$D(1D_2)K$	5.45	2.18
	$D(1^3D_3)K$	34.0	13.6
	$D_s(2^3S_1)\eta$	5.10	2.04
	$D_s(1^3D_3)\eta$	7.24	2.89
	Total	250.3	100
$D_s(2^3F_4)$ 3544	DK	3.59	2.54
	D^*K	0.254	0.179
	D^*K^*	32.4	22.9
	$D(2^1S_0)K$	10.8	7.63
	$D(2^3S_1)K$	10.6	7.49
	$D(1^3P_0)K^*$	3.04	2.15
	$D(1P_1)K$	11.2	7.91
	$D(1P_1)K^*$	3.38	2.39
	$D(1P_1')K$	4.94	3.49
	$D(1P_1')K^*$	5.03	3.55
	$D(1^3P_2)K$	10.4	7.35
	$D(1^3P_2)K^*$	29.6	20.9
	$D(1D_2')K$	2.90	2.05
	$D(1^3D_3)K$	5.32	3.76
	Total	141.5	100

[24,29–32,84,95,96,99] with a relatively small $2^3S_1 - 1^3D_1$ mixing angle of ~10° [31]. A consequence of this identification is that there are another three excited D_s states in this mass region to be found; the spin-singlet partner of the $D_{s1}^*(2709)^\pm$ is expected to lie ~60 MeV lower in mass with $M(2^1S_0(c\bar{s})) \sim 2650$ MeV, a width of ~78 MeV and decaying to D^*K [31]. The $J = 2$ states using the predicted $1D$ mass splittings relative to the 1^3D_3 mass give $M(D_2') \sim 2872$ MeV and $M(D_2) \sim 2846$ MeV with the partial widths given in Table XLVII which were taken from Ref. [31]. We note that in the HQL we expect one of the $J = 2$ states to be degenerate with the 1^3D_3 and relatively narrow while the other $J = 2$ state is expected to be degenerate with the 1^3D_1 and relatively broad which is consistent with our results. It will be interesting to see what experiment has to say about these states.

B. The $D_{sJ}(3044)^\pm$ state

The remaining new state is the $D_{sJ}(3044)^\pm$. This state has been studied by a number of authors [24,28,81,84,94,100]. We start by noting that it has only been seen by one experiment, *BABAR* [5], albeit with 6.0 standard deviation statistical significance. It has only been seen in the D^*K final state implying it is of unnatural parity: 0^-, 1^+, 2^-, 3^+, 4^-, etc. Of all the states with these quantum numbers the predicted masses for the $2P_1'$ and $2P_1$ states are closest to the observed mass, 3038 and 3018 MeV respectively. The $2P_1$ is expected to have a total width of 143 MeV and a BR to the D^*K final state of 43% while the

TABLE XLI. Partial widths and branching ratios for strong decays for the $1G$ charm-strange mesons. See the caption for Table IV for further explanations.

Initial state	Final state	Width (MeV)	BR (%)
$D_s(1^3G_3)$	DK	22.0	6.70
3469	DK^*	20.5	6.24
	D^*K	22.3	6.79
	D^*K^*	47.4	14.4
	$D(2^1S_0)K$	7.27	2.21
	$D(2^3S_1)K$	3.76	1.15
	$D(1P_1)K$	66.5	20.3
	$D(1P_1)K^*$	16.6	5.06
	$D(1^3P_2)K$	19.6	5.97
	$D(1D_2)K$	65.6	20.0
	$D_s\eta$	3.46	1.05
	$D_s(1P_1)\eta$	9.54	2.91
	Total	328.4	100
$D_s(1G_4)$	DK^*	45.0	23.9
3436	D^*K	43.8	23.2
	D^*K^*	51.0	27.0
	$D(1^3P_0)K$	2.51	1.33
	$D(1P_1)K$	4.09	2.17
	$D(1P_1)K^*$	21.1	11.2
	$D(1P_1')K$	2.34	1.24
	$D(1^3P_2)K$	4.64	2.46
	$D_s\phi$	5.59	2.96
	$D_s^*\eta$	2.20	1.17
	$D_s^*\phi$	2.87	1.52
	Total	188.6	100
$D_s(1G_4')$	DK^*	24.0	6.77
3469	D^*K	50.2	14.2
	D^*K^*	56.8	16.0
	$D(2^3S_1)K$	10.1	2.85
	$D(1P_1)K$	5.03	1.42
	$D(1^3P_2)K$	92.9	26.2
	$D(1^3P_2)K^*$	9.96	2.81
	$D(1^3D_3)K$	74.9	21.1
	$D_s^*\eta$	6.94	1.96
	$D_s^*\phi$	3.73	1.05
	$D_s(1^3P_2)\eta$	11.9	3.36
	Total	354.5	100
$D_s(1^3G_5)$	DK	23.1	12.8
3433	DK^*	10.4	5.77
	D^*K	24.0	13.3
	D^*K^*	92.3	51.2
	$D(1P_1)K$	3.59	1.99
	$D(1P_1')K$	2.91	1.61
	$D(1^3P_2)K$	7.31	4.05
	$D(1^3P_2)K^*$	5.38	2.98
	$D_s^*\phi$	6.10	3.38
	Total	180.4	100

TABLE XLII. Partial widths and branching ratios for strong decays for the 2^3G_3 and $2G_4$ charm-strange mesons. See the caption for Table IV for further explanations.

Initial state	Final state	Width (MeV)	BR (%)
$D_s(2^3G_3)$	DK	12.4	4.33
3789	DK^*	8.94	3.13
	D^*K	11.0	3.85
	D^*K^*	6.34	2.22
	$D(2^1S_0)K^*$	6.73	2.35
	$D(2^3S_1)K^*$	13.5	4.72
	$D(3^1S_0)K$	3.30	1.15
	$D(1P_1)K$	22.3	7.80
	$D(1P_1)K^*$	7.74	2.71
	$D(1P_1')K^*$	7.10	2.48
	$D(1^3P_2)K$	5.18	1.81
	$D(1^3P_2)K^*$	14.8	5.17
	$D(2P_1)K$	16.0	5.59
	$D(2^3P_2)K$	8.25	2.88
	$D(1D_2)K$	23.9	8.36
	$D(1D_2)K^*$	16.2	5.66
	$D(1^3D_3)K$	8.63	3.02
	$D(2D_2)K$	31.3	10.9
	$D(1F_3)K$	18.5	6.47
	$D_s(2P_1)\eta$	5.15	1.80
	$D_s(1F_3)\eta$	6.52	2.28
	Total	286.0	100
$D_s(2G_4)$	DK^*	20.3	10.2
3759	D^*K	4.70	2.36
	D^*K^*	13.9	6.99
	$D(2^1S_0)K^*$	14.7	7.39
	$D(2^3S_1)K$	21.1	10.6
	$D(2^3S_1)K^*$	14.0	7.04
	$D(1P_1)K^*$	10.5	5.28
	$D(1P_1')K^*$	6.37	3.20
	$D(1^3P_2)K$	17.4	8.75
	$D(1^3P_2)K^*$	10.2	5.13
	$D(2^3P_0)K$	2.07	1.04
	$D(2P_1)K$	3.09	1.55
	$D(2^3P_2)K$	3.35	1.68
	$D(1^3D_1)K$	2.86	1.44
	$D(1D_2)K$	3.52	1.77
	$D(1D_2)K^*$	27.2	13.7
	$D(1^3D_3)K$	4.25	2.14
	$D(1^3D_3)K^*$	2.33	1.17
	Total	198.9	100

$2P_1'$ is expected to have a total width of 148 MeV with BR to D^*K of 25%. The experimental error on the width is quite large, $\sim\pm 55$ MeV, and there is considerable theoretical uncertainty on the predicted width which could be up to a factor of 2. As a consequence, the $D_{sJ}(3044)^{\pm}$

TABLE XLIII. Partial widths and branching ratios for strong decays for the $2G'_4$ and 2^3G_5 charm-strange mesons. See the caption for Table IV for further explanations.

Initial state	Final state	Width (MeV)	BR (%)
$D_s(2G'_4)$ 3790	DK^*	3.65	1.20
	D^*K	26.1	8.57
	D^*K^*	14.9	4.89
	$D(2^1S_0)K^*$	6.80	2.23
	$D(2^3S_1)K^*$	16.7	5.48
	$D(3^3S_1)K$	4.11	1.35
	$D(1P_1)K^*$	7.61	2.50
	$D(1P'_1)K^*$	6.88	2.26
	$D(1^3P_2)K$	30.6	10.0
	$D(1^3P_2)K^*$	15.5	5.09
	$D(2P_1)K$	3.80	1.25
	$D(2^3P_2)K$	23.8	7.82
	$D(1D_2)K$	4.16	1.37
	$D(1^3D_3)K$	30.3	9.95
	$D(1^3D_3)K^*$	19.5	6.40
	$D(2^3D_3)K$	30.6	10.0
	$D(1^3F_4)K$	21.5	7.06
	$D_s(2^3P_2)\eta$	5.74	1.88
	$D_s(1^3F_4)\eta$	7.21	2.37
	Total	304.5	100
$D_s(2^3G_5)$ 3757	DK	7.33	3.83
	DK^*	1.80	0.941
	D^*K	3.65	1.91
	D^*K^*	33.7	17.6
	$D(2^1S_0)K$	8.90	4.65
	$D(2^1S_0)K^*$	2.39	1.25
	$D(2^3S_1)K$	10.9	5.70
	$D(2^3S_1)K^*$	26.1	13.6
	$D(1P_1)K$	7.03	3.68
	$D(1P_1)K^*$	3.84	2.01
	$D(1P'_1)K^*$	5.13	2.68
	$D(1^3P_2)K$	5.24	2.74
	$D(1^3P_2)K^*$	12.6	6.59
	$D(2P_1)K$	2.72	1.42
	$D(2P'_1)K$	2.69	1.41
	$D(2^3P_2)K$	4.69	2.45
	$D(1D_2)K$	2.24	1.17
	$D(1D'_2)K$	3.87	2.02
	$D(1^3D_3)K$	5.76	3.01
	$D(1^3D_3)K^*$	24.9	13.0
	$D_s(1^3P_2)\phi$	3.98	2.08
	Total	191.2	100

could be either state. Referring to Table XXIX the DK^* final state might be a useful discriminator between these two possibilities; the $2P'_1$ is predicted to have a BR of 22% to DK^* while for the $2P_1$ it is predicted to be 5%. Another possibility is that, because the states are relatively close together and broad, perhaps *BABAR* observed two overlapping states. A means of discriminating between these possibilities is to measure BRs to different final states. For example, we estimate that the branching ratios of the $D_{s1}(2P'_1)$ to DK^* and $D_s\phi$ are 22% and 2.8% respectively versus 43% and 11.3% respectively for the $D_{s1}(2P_1)$. Measurement of BRs to these final states would provide a good discriminator for these possibilities (see also Ref. [24,81,84,100]). A final possibility is that the observed state does decay to DK but that it simply was not observed. The $D^*_{s2}(2^3P_2)$ state is predicted to have a mass ~3048 MeV and total width of 132 MeV with BRs to D^*K and DK of 23% and 6.5% respectively. It may have been that the signal in the DK final state was simply too small to see with limited statistics.

While we consider it most likely that the $D_{sJ}(3044)^{\pm}$ is a member of the $2P(c\bar{s})$ multiplet we mention other possibilities for completeness. Other unnatural parity states with masses not too far from the $D_{sJ}(3044)^{\pm}$ are the $1F_3$ with $M = 3186$ MeV and $\Gamma = 183$ MeV, the $1F'_3$ with $M = 3218$ MeV and $\Gamma = 323$ MeV, the $2D_2$ with $M = 3298$ MeV and $\Gamma = 106$ MeV and the $2D'_2$ with $M = 3323$ MeV and $\Gamma = 203$ MeV. However we consider all of these possibilities unlikely as the predicted masses are over 100 MeV from the observed mass. And although it would not surprise us if our predictions were off by several tens of MeV we do not expect them to be off by over 100 MeV. A final possibility is the 3^1S_0 with $M = 3154$ MeV and $\Gamma = 79$ MeV with BR to D^*K of 15%. In this case the predicted width is smaller by a factor of three so that it seems unlikely that the $D_{sJ}(3044)^{\pm}$ could be identified as the 3^1S_0.

To summarize, with the information we currently have for the $D_{sJ}(3044)^{\pm}$ it is most likely either the $D_{s1}(2P'_1)$ or the $D_{s1}(2P_1)$ or both states overlapping. This conclusion is consistent with other studies [17,24,81,83,84,94,100]. Another possibility is that it is $D^*_{s2}(2^3P_2)$ with the signal for the DK final state too small to be observed with current statistics. These different possibilities can be tested by measuring BRs to DK^* and $D_s\phi$ final states. We also expect that it should be possible to observe the $2P$ partners which will lie in this mass region in DK and D^*K^* final states.

VII. FINDING THE MISSING CHARM MESONS

The key to observing missing states is that their total width is not too large and that the BRs to at least some simple final states are not too small. This is how the new charm states were found by the *BABAR* and LHCb collaborations. Thus, we can use our tables of charm meson properties to identify candidate states that could be observed in the near future. As the states become more massive, more and more channels open up so that the BRs to easier to observe final states become smaller and smaller. For masses above around 3500 MeV for charm mesons the BRs to simple final states are less than 1% and are likely too small to observe. For charm-strange mesons, BRs to at least

TABLE XLIV. Recently observed charm mesons. The first uncertainty is statistical, the second is due to systematic uncertainties and the third when included is for model dependent uncertainties.

State	J^P	Observed Decays	Mass (MeV)	Width (MeV)	References
$D_J(2550)^0$	0^-	$D^{*+}\pi^-$	$2539.4 \pm 4.5 \pm 6.8$	$130 \pm 12 \pm 13$	*BABAR* [2]
$D_J(2580)^0$		$D^{*+}\pi^-$	$2579.5 \pm 3.4 \pm 3.5$	$177.5 \pm 17.8 \pm 46.0$	LHCb [11]
$D_J^*(2600)^0$		$D^+\pi^-$	$2608.7 \pm 2.4 \pm 2.5$	$93 \pm 6 \pm 13$	*BABAR* [2]
				$\Gamma(\to D^+\pi^-)/\Gamma(\to D^{*+}\pi^-) = 0.32 \pm 0.02 \pm 0.09$	*BABAR* [2]
$D_J^*(2650)^0$		$D^{*+}\pi^-$	$2649.2 \pm 3.5 \pm 3.5$	$140.2 \pm 17.1 \pm 18.6$	LHCb [11]
$D_J(2750)^0$		$D^{*+}\pi^-$	$2752.4 \pm 1.7 \pm 2.7$	$71 \pm 6 \pm 11$	*BABAR* [2]
$D_J(2740)^0$		$D^{*+}\pi^-$	$2737.0 \pm 3.5 \pm 11.2$	$73.2 \pm 13.4 \pm 25.0$	LHCb [11]
$D_J^*(2760)^0$		$D^{*+}\pi^-$	$2761.1 \pm 5.1 \pm 6.5$	$74.4 \pm 3.4 \pm 37.0$	LHCb [11]
		$D^+\pi^-$	$2760.1 \pm 1.1 \pm 3.7$	$74.4 \pm 3.4 \pm 19.1$	LHCb [11]
		$D^+\pi^-$	$2763.3 \pm 2.3 \pm 2.3$	$60.9 \pm 5.1 \pm 3.6$	*BABAR* [2]
				$\Gamma(\to D^+\pi^-)/\Gamma(\to D^{*+}\pi^-) = 0.42 \pm 0.05 \pm 0.11$	*BABAR* [2]
$D_J^*(2760)^+$		$D^0\pi^+$	$2771.7 \pm 1.7 \pm 3.8$	$66.7 \pm 6.6 \pm 10.5$	LHCb [11]
$D_1^*(2760)^0$	1^-	$D^+\pi^-$	$2781 \pm 18 \pm 11 \pm 6$	$177 \pm 32 \pm 20 \pm 7$	LHCb [9]
$D_3^*(2760)^-$	3^-	$\bar{D}^0\pi^-$	$2798 \pm 7 \pm 1 \pm 7$	$105 \pm 18 \pm 6 \pm 23$	LHCb [10][a]
$D_J(3000)^0$		$D^{*+}\pi^-$	2971.8 ± 8.7	188.1 ± 44.8	LHCb [11]
$D_J^*(3000)^0$		$D^+\pi^-$	3008.1 ± 4.0	110.5 ± 11.5	LHCb [11]

[a]We quote the results from the isobar analysis.

some simple final states remain non-negligible for all states we consider due to the smaller phase space because of the larger kaon mass relative to that of the pion. Another consideration is that states within multiplets will be overlapping and states in different multiplets are close enough in mass that it will require more than "bump hunting" to classify newly found states. Determining the spin of a state and measuring BRs to multiple final states will be important to disentangle the spectrum. We have already seen examples of this in the preceding sections.

A. The charm mesons

For the most part, the recently observed states are the states with large BRs to simple final states. For example the predicted BRs of the 2^3S_1 and 2^1S_0 to the observed final state $D^*\pi$ are 58% and 99% respectively. Likewise the $1D$ states have BRs to $D^*\pi$ ranging from 13% to 38% and the 1^3F_4 has a BR to $D\pi$ of 12%. We use BRs to simple final states to identify good candidates for discovery.

We start with the $1D$ multiplet. Three of the states have been observed, the 1^3D_1 and 1^3D_3 and tentatively the $1D_2$ leaving only the $1D_2'$ to be found. This state has a BR of 38% to $D^*\pi$ but is predicted to be rather broad, ~240 MeV, making it potentially difficult to disentangle from the other three $1D$ states in that mass region. This state might also be seen in the D_s^*K final state.

We tentatively identified the 3^1S_0 state with the $D_J(3000)$ although the $1F_3$ and $1F_3'$ are also possibilities. If we accept the 3^1S_0 assignment we would expect that the 3^3S_1 should also be seen with comparable statistics. The distinguishing feature is that the 3^3S_1 should be seen in both $D\pi$ and $D^*\pi$ final states. Even if the $D_J(3000)$ turns out to be the $1F_3$ or $1F_3'$ we expect that the $3S$ states could be seen in the near future.

The $2P$ states also have relatively large BRs to $D^*\pi$ and $D\pi$ final states. Their masses are expected to be in the 2900–2950 MeV mass range with widths ranging from 114 to 212 MeV. In fact, some have argued that the 2^3P_0 can be identified with the $D_J^*(3000)$. We expect that the $2P$ multiplet can be observed in $D^*\pi$ and $D\pi$ final states. The four states are only split by 37 MeV so that it will require the measurement into different final states to uniquely identify the individual states. As we pointed out previously, in addition to $D^*\pi$ and $D\pi$, the $D\rho$ final state will be a useful discriminator. Other final states which would help are the D_sK, D_s^*K, D_sK^* and $D^*\rho$ although in some cases they only have a sizeable BR for one of the $2P$ states. In this case their observation in one of these final states would eliminate other possibilities.

The $1F$ multiplet is next in line using this criteria for "discoverability" with BRs to $D\pi$ and $D^*\pi$ ranging from 8% to 20%. Their masses are around 3100 MeV with predicted widths ranging from 126 to 270 MeV. Depending on the reliability of our width predictions, the two broad states, the 1^3F_2 and $1F_3'$, are likely too broad to be easily seen. We have tentatively identified the 1^3F_4 with the $D_J^*(3000)$ state leaving the $1F_3$ to be found. If found, it is expected to have a large BR to $D\rho$ which could be used as confirmation.

The $1G$ multiplet also has a significant BR to the $D\pi$ and $D^*\pi$ final states ranging from 4% to 17% depending on the state. Their masses range from around 3360 to 3400 MeV and their widths range from 118 to 254 MeV. The narrower widths correspond to the $j = 9/2$ doublet and the broader

TABLE XLV. Properties of the $2P$, $3S$, and $1F$ charm meson multiplets. The predicted masses listed here have been shifted down by 34 MeV, the difference between the predicted and measured D^* masses. We list BRs of the simplest final states and in some cases final states with the largest BRs. Blank entries represent either forbidden decays or BRs too small to be included.

			Branching ratios (%)									
State	Mass (MeV)	Width (MeV)	$D\pi$	$D^*\pi$	$D\rho$	$D^*\rho$	$D\omega$	$D^*\omega$	D_sK	D_s^*K	D_sK^*	$D_s^*K^*$
						Natural parity states						
2^3P_2	2923	114	4.4	15	9.3	23	3.0	8.1	3.2	4.9	0.3	
2^3P_0	2897	190	13.4			16.8		5.4	0.4			
3^3S_1	3076	103	3.1	5.4	0.8	3.2	0.2	1.3		0.6	0.9	6.3
1^3F_4	3079	129	12.2	11.8	3.1	45.7	1.0	14.8	0.8	0.6		1.2
1^3F_2	2098	243	9.5	7.6	6.7	6.6	2.2	2.1	3.3	2.1	0.8	0.2
						Unnatural parity states						
$2P_1$	2890	125		30.3	2.7	19.3	0.9	6.5		7.2	11.4	
$2P_1'$	2924	212		10.2	8.9	11		3.5		2.1	1.9	
3^1S_0	3034	106		4.9		9.3		3.3		2.3	2.2	3.2
$1F_3'$	3109	269		17.2	3.6	11.0	1.2	3.6		5.2		0.4
$1F_3$	3074	126		20	31	20.3	10.2	6.6		0.9	3.3	0.4

widths to the $j = 7/2$ doublet. We expect it is more likely that the narrower 1^3G_5 and $1G_4$ states will be observed first. The natural parity 1^3G_5 decays to both $D\pi$ and $D^*\pi$ while the unnatural $1G_4$ can only decay to $D^*\pi$. Other decay modes that can be used to distinguish between these states are $D\rho$ where $\mathrm{BR}(D(1^3G_5) \to D\rho) \simeq 3\%$ versus $\mathrm{BR}(D(1G_4) \to D\rho) \simeq 15\%$ and $D^*\rho$ where $\mathrm{BR}(D(1^3G_5) \to D^*\rho) \simeq 32\%$ versus $\mathrm{BR}(D(1G_4) \to D^*\rho) \simeq 17\%$. One could use similar measurements to identify the $1G_4'$ and 1^3G_3.

Beyond these multiplets, the BRs to $D\pi$ and $D^*\pi$ final states for the most part become relatively small and other final states become more important for finding higher excited missing states. We already suggested that the $D\rho$ and $D^*\rho$ final states would be useful for identifying excited charm states and for many of the higher excited states they have the largest BRs and could prove crucial for their discovery. For example, in the $2D$ multiplet $\mathrm{BR}(2^3D_1 \to D\pi) \simeq 5.1\%$ but $\mathrm{BR}(2^3D_1 \to D^*\rho) \simeq 13.9\%$. The challenge is that the D^* and ρ have to be reconstructed with numerous pions in the final state. Similarly, $\mathrm{BR}(2^3D_3 \to D^*\rho) \simeq 11.4\%$ versus $\mathrm{BR}(2^3D_3 \to D^*\pi) \simeq 3.0\%$ and $\mathrm{BR}(2D_2 \to D^*\rho) \simeq 14.7\%$ versus $\mathrm{BR}(2D_2 \to D^*\pi) \simeq 9.5\%$. To complete the multiplet we note that $\mathrm{BR}(2D_2' \to D^*\rho) \simeq 7.3\%$ versus $\mathrm{BR}(2D_2' \to D^*\pi) \simeq 7.8\%$ so that the ratio $\mathrm{BR}(2D_2^{(\prime)} \to D^*\rho)/\mathrm{BR}(2D_2^{(\prime)} \to D^*\pi)$ could be useful for discriminating between $2D_2'$ and $2D_2$.

One can continue this exercise by examining the predicted BRs of higher mass multiplets given in Tables V–XXIV. Further examples that satisfy the criteria of being not too broad while having a not too small BR to a simple final state like $D\pi$ and $D^*\pi$ are members of the $2D$ and $3P$ multiplets etc. The interested reader can identify more candidate states that might be found in the near future by examining Tables V–XXIV.

B. The charm-strange mesons

We follow the approach used in the previous section to identify likely charm-strange discovery candidates using the criteria that states with large branching ratios to simple final states are the ones most likely to be observed.

The charm-strange states that have recently been observed by Belle, *BABAR* and LHCb all follow this pattern of large BRs to simple states. For example, the $D_{s1}^*(2709)$ identified as the $D_s^*(2^3S_1)$ is predicted to have $\mathrm{BR}(D_s^*(2^3S_1) \to D^*K) \simeq 58.6\%$ and $\mathrm{BR}(D_s^*(2^3S_1) \to DK) \simeq 32.5\%$, the discovery channels. Similarly the $D_{s1}^*(2860)$ and $D_{s3}^*(2860)$ are identified as the $D_s^*(1^3D_1)$ and $D_s^*(1^3D_3)$ which are predicted to have BRs to DK, the channel studied by LHCb, of 47.3% and 57.7% respectively. Finally, we tentatively identify the $D_{sJ}(3044)$ as either $2P_1$ or $2P_1'$ whose calculated BRs to D^*K, the *BABAR* discovery channel, are 42.9% and 24.7% respectively. The common thread is that all of the recently discovered $D_{sJ}^{(*)}$ have large BRs to simple final states.

If we extrapolate this to other excited states we can expect many more $D_{sJ}^{(*)}$ to be discovered in the near future. The singlet partner of the $D_{s1}^*(2709)$, the $D_s(2^1S_0)$, is expected to lie 59 MeV lower at 2650 MeV with a width of 74 MeV and a BR of almost 100% to D^*K. The $J = 2$ partners of $D_{s1}^*(2860)$ and $D_{s3}^*(2860)$ are the $1D_2$ and $1D_2'$, which should lie very close in mass to the D_{s1}^* and D_{s3}^*. Their widths are expected to be 115 and 195 MeV respectively with BRs to D^*K of 18.3% and 83.4%. Finally, if the $D_{sJ}(3044)$ is the $2P_1$ or $2P_1'$ there will be three other $2P$ partner states, the 2^3P_2, 2^3P_0, and the other $J = 1$ state. Because we did not determine if the $D_{sJ}(3044)$ is the $2P_1$ or $2P_1'$ we make a few comments about all four of the $2P$ states and refer to Table XXIX for details. All four of the $2P$ states are close in mass ranging from 3005 MeV for the 2^3P_0 to 3048 MeV for the 2^3P_2 state. The widths of

TABLE XLVI. The recently observed charm-strange mesons. The first uncertainty is statistical, the second is due to experimental systematic effects and the third, when given, is due to model variations.

State	J^P	Observed Decays	Mass (MeV)	Width (MeV)	References
$D^*_{s1}(2700)^+$	1^-	D^0K^+	2699^{+14}_{-7}	127^{+24}_{-19}	*BABAR* [6]
				$\frac{\Gamma(D^*K)}{\Gamma(DK)} = 0.91 \pm 0.13 \pm 0.12$	*BABAR* [5]
$D^*_{s1}(2700)^+$	1^-	D^+K^0 and D^0K^+	$2709.2 \pm 1.9 \pm 4.5$	$115.8 \pm 7.3 \pm 12.1$	LHCb [12]
$D^*_{sJ}(2860)^+$		DK and D^*K	$2863.2^{+4.0}_{-2.6}$	58 ± 11	PDG [7]
$D^*_{sJ}(2860)^+$		DK and D^*K	$2862 \pm 2^{+5}_{-2}$	$48 \pm 3 \pm 6$	*BABAR* [5]
				$\frac{\Gamma(D^*K)}{\Gamma(DK)} = 1.10 \pm 0.15 \pm 0.19$	*BABAR* [5]
$D^*_{s1}(2860)^-$	1^-	$\bar{D}^0K^-$	$2859 \pm 12 \pm 6 \pm 23$	$159 \pm 23 \pm 27 \pm 72$	LHCb [13,14]
$D^*_{s3}(2860)^-$	3^-	$\bar{D}^0K^-$	$2860.5 \pm 2.6 \pm 2.5 \pm 6.0$	$53 \pm 7 \pm 4 \pm 6$	LHCb [13,14]
$D_{sJ}(3044)^+$		D^*K	$3044 \pm 8^{+30}_{-8}$	$239 \pm 35^{+46}_{-42}$	*BABAR* [5]

all four states are around 130–150 MeV. What distinguishes them are their BRs to different final states: $D^*_s(2^3P_0)$ decays to DK with BR $\simeq 35\%$ but does not decay to D^*K, while the $D_s(2P_1)$ and $D_s(2P'_1)$ decay to D^*K with BR $\simeq 42.9\%$ and 24.7% respectively but do not decay to DK, and $D^*_s(2^3P_2)$ can decay to both DK and D^*K with BRs of 6.5% and 23.4% respectively. The point is that all of these states have sizeable BRs to final states that have already led to the observation of a new state in this mass region so that we expect that the remaining three states should also be seen.

So far we have only discussed charm-strange mesons that are members of multiplets with states that have already been observed. The next most promising states to find are likely to be members of the $1F$ multiplet and in fact the $1F_3$ states are alternative possibilities for the $D_{sJ}(3044)$. We leaned towards the $2P_1$ identification primarily because the predicted mass was closer to the observed mass. In any case the $1F$ states are expected to sit around 3200 MeV. The 1^3F_4 is predicted to have a width of 182 MeV with BRs to DK and D^*K of 15.9% and 13.6% respectively, the $1F_3$ and $1F'_3$ have widths of 183 MeV and 323 MeV respectively with BRs to D^*K of 22.6% and 28.9% respectively and do not decay to DK, and the 1^3F_2 is predicted to have a width of 292 MeV and decays to DK and D^*K with BRs of 15.3% and 12.9% respectively. Although the BRs are all sizeable, the $1F$ states are expected to be relatively broad so it is not clear if they will be observed in the near future. However, as we have repeatedly pointed out, our width predictions can easily be off by up to a factor of two so that if they turn out to be narrower than we predict, their observation would be more likely.

We note that the $1G$ multiplet has similar BRs to final states (see Table XLI) as the $1F$ multiplet so it might also be possible to observe these states with the same caveat regarding their large total widths. It would be extremely interesting to find these states as we would then have a series of angular momentum states stretching from $L = 0$ to $L = 4$ which would test the linearity of the Regge trajectory and thus the linearity of the confining potential [45]. If large deviations were found it would also provide some insights into the importance of meson loop contributions to the mass of excited states.

Beyond these states there are a smattering of states that have large BRs to the DK and D^*K final states we have focused on. A few examples are the 3^3P_0 with a predicted mass of 3412 MeV, width of 104 MeV and BR to DK of 19.5%, the 4^3P_0 with $M = 3764$ MeV, $\Gamma = 105$ MeV and BR to DK of 10%, the $2D_2$ with $M = 3298$ MeV, $\Gamma = 106$ MeV and BR to D^*K of 11.4% and the $2D'_2$ with $M = 3323$ MeV, $\Gamma = 203$ MeV and BR to D^*K of 21.4%. One can turn to Tables XXXI–XLIII to explore further possibilities. As more measurements are made we will be able to gauge the reliability of our predictions and those of others and refine the models to improve their predictive power.

TABLE XLVII. Partial widths for the $1D_2$ and $1D'_2$ $c\bar{s}$ mesons calculated using the $^3P_0$ quark-pair-creation model from Ref. [31]. The $1D_2$ and $1D'_2$ masses listed here and used to calculate the partial widths were obtained by subtracting the predicted splittings from the measured 1^3D_3 mass.

State	Property	Predicted (MeV)
$D_s(D'_2)$	Mass	2872
	$D'_{s2} \to D^*K$	159
	$D'_{s2} \to DK^*$	4.4
	$D'_{s2} \to D^*K^*$	0
	$D'_{s2} \to D^*_s\eta$	21
	Γ_{Total}	184
$D_s(D_2)$	Mass	2846
	$D_{s2} \to D^*K$	16
	$D_{s2} \to DK^*$	58
	$D_{s2} \to D^*K^*$	0
	$D_{s2} \to D^*_s\eta$	0.4
	Γ_{Total}	75

VIII. SUMMARY

In this paper we calculated the properties of charm and charm-strange mesons using the relativized quark model to calculate masses and wave functions which were used to calculate radiative transition partial widths. We calculated hadronic widths using the quark pair creation model with simple harmonic oscillator wave functions with the oscillator parameters fitted to the rms radius of the relativized quark model wave functions.

We used our results to identify recently observed charm and charm-strange mesons in terms of quark model spectroscopic states. Our results support the previously made assignment of the $D_J(2550)^0$ and $D_J^*(2600)^0$ as the $2^1S_0(c\overline{q})$ and $2^3S_1(c\overline{q})$ states respectively. We identify the $D_1^*(2760)^0$ and $D_3^*(2760)^0$ as the $1^3D_1(c\overline{q})$ and $1^3D_3(c\overline{q})$ respectively and tentatively identify the $D_J(2750)^0$ as the $1D_2(c\overline{q})$ state. In the latter case further measurements are needed to strengthen the assignment. We suggested that measurements of BRs to $D\rho$ and $D^*\pi$ would be useful. We tentatively identified the $D_J^*(3000)^0$ as the $D_4^*(1^3F_4)$ state and favor the $D_J(3000)^0$ to be the $D(3^1S_0)$ although we do not rule out the $1F_3$ and $1F_3'$ assignments. For the recently observed charm-strange mesons we identify the $D_{s1}^*(2709)^{\pm}$, $D_{s1}^*(2860)^-$, and $D_{s3}^*(2860)^-$ as the $2^3S_1(c\overline{s})$, $1^3D_1(s\overline{c})$, and $1^3D_3(s\overline{c})$ respectively and suggest that the $D_{sJ}(3044)^{\pm}$ is most likely the $D_{s1}(2P_1')$ or $D_{s1}(2P_1)$ although it might be the $D_{s2}^*(2^3P_2)$ with the DK final state too small to be observed with current statistics.

Finally we suggested excited charm and charm-strange mesons that might be seen in the near future based on the criteria that they do not have too large a total width and they have a reasonable branching ratio to simple final states. We expect that our results comprised of tables of masses, widths and BRs will be useful to this end.

While we have shown the usefulness of our results in identifying newly discovered states we are equally keen that they be a useful guide for future searches for missing states.

ACKNOWLEDGMENTS

This research was supported in part by the Natural Sciences and Engineering Research Council of Canada under Grant No. 121209-2009 SAPIN.

[1] A. J. Bevan *et al.* (*BABAR* and Belle Collaborations), The physics of the B factories, Eur. Phys. J. C **74**, 3026 (2014).
[2] P. del Amo Sanchez *et al.* (*BABAR* Collaboration), Observation of new resonances decaying to $D\pi$ and $D^*\pi$ in inclusive e^+e^- collisions near $\sqrt{s} = 10.58$ GeV, Phys. Rev. D **82**, 111101 (2010).
[3] B. Aubert *et al.* (*BABAR* Collaboration), Observation of a New D_s Meson Decaying to DK at a Mass of 2.86 GeV/c^2, Phys. Rev. Lett. **97**, 222001 (2006)].
[4] J. Brodzicka *et al.* (Belle Collaboration), Observation of a New D_{sJ} Meson in $B^+ \to \overline{D}^0 D^0 K^+$ Decays, Phys. Rev. Lett. **100**, 092001 (2008).
[5] B. Aubert *et al.* (*BABAR* Collaboration), Study of D_{sJ} decays to D^*K in inclusive e^+e^- interactions, Phys. Rev. D **80**, 092003 (2009).
[6] J. P. Lees *et al.* (*BABAR* Collaboration), Dalitz plot analyses of $B^0 \to D^- D^0 K^+$ and $B^+ \to \overline{D}^0 D^0 K^+$ decays, Phys. Rev. D **91**, 052002 (2015).
[7] K. A. Olive *et al.* (Particle Data Group Collaboration), Review of particle physics, Chin. Phys. C **38**, 090001 (2014).
[8] D. Besson *et al.* (CLEO Collaboration), Observation of a narrow resonance of mass 2.46 GeV/c^2 decaying to $D_s^{*+}\pi^0$ and confirmation of the $D_{sJ}^*(2317)$ state, Phys. Rev. D **68**, 032002 (2003); **75**, 119908 (2007).
[9] R. Aaij *et al.* (LHCb Collaboration), First observation and amplitude analysis of the $B^- \to D^+ K^- \pi^-$ decay, Phys. Rev. D **91**, 092002 (2015).
[10] R. Aaij *et al.* (LHCb Collaboration), Dalitz plot analysis of $B^0 \to \overline{D}^0 \pi^+ \pi^-$ decays, Phys. Rev. D **92**, 032002 (2015).
[11] R. Aaij *et al.* (LHCb Collaboration), Study of D_J meson decays to $D^+\pi^-$, $D^0\pi^+$ and $D^{*+}\pi^-$ final states in pp collision, J. High Energy Phys. 09 (2013) 145.
[12] R. Aaij *et al.* (LHCb Collaboration), Study of D_{sJ} decays to D^+K_S and D^0K^+ final states in pp collisions, J. High Energy Phys. 10 (2012) 151.
[13] R. Aaij *et al.* (LHCb Collaboration), Observation of Overlapping Spin-1 and Spin-3 $\overline{D}^0K^-$ Resonances at Mass 2.86 GeV/c^2, Phys. Rev. Lett. **113**, 162001 (2014).
[14] R. Aaij *et al.* (LHCb Collaboration), Dalitz plot analysis of $B_s^0 \to \overline{D}^0 K^- \pi^+$ decays, Phys. Rev. D **90**, 072003 (2014).
[15] Z. G. Wang, $D_{s3}^*(2860)$ and $D_{s1}^*(2860)$ as the 1D $c\overline{s}$ states, Eur. Phys. J. C **75**, 25 (2015).
[16] P. Colangelo, F. De Fazio, and S. Nicotri, $D_{sJ}(2860)$ resonance and the $s_\ell^P = 5/2^- c\overline{s}(c\overline{q})$ doublet, Phys. Lett. B **642**, 48 (2006).
[17] L. Y. Xiao and X. H. Zhong, Strong decays of higher excited heavy-light mesons in a chiral quark model, Phys. Rev. D **90**, 074029 (2014).
[18] H. W. Ke, J. H. Zhou, and X. Q. Li, Study on radiative decays of $D_{sJ}^*(2860)$ and $D_{s1}^*(2710)$ into D_s by means of LFQM, Eur. Phys. J. C **75**, 28 (2015).
[19] Q. T. Song, D. Y. Chen, X. Liu, and T. Matsuki, $D_{s1}^*(2860)$ and $D_{s3}^*(2860)$: candidates for $1D$ charmed-strange mesons, Eur. Phys. J. C **75**, 30 (2015).

[20] Q. T. Song, D. Y. Chen, X. Liu, and T. Matsuki, Higher radial and orbital excitations in the charmed meson family, Phys. Rev. D **92**, 074011 (2015).

[21] Y. Sun, X. Liu, and T. Matsuki, Newly observed $D_J(3000)^{+,0}$ and $D_J^*(3000)^0$ as $2P$ states in D meson family, Phys. Rev. D **88**, 094020 (2013).

[22] B. Zhang, X. Liu, W.-Z. Deng, and S.-L. Zhu, $D_{sJ}(2860)$ and $D_{sJ}(2715)$, Eur. Phys. J. C **50**, 617 (2007).

[23] G. L. Yu, Z. G. Wang, Z. Y. Li, and G. Q. Meng, Systematic analysis of the $D_J(2580)$, $D_J^*(2650)$, $D_J(2740)$, $D_J^*(2760)$, $D_J(3000)$ and $D_J^*(3000)$ in D meson family, Chin. Phys. C **39**, 063101 (2015).

[24] D. M. Li, P. F. Ji, and B. Ma, The newly observed open-charm states in quark model, Eur. Phys. J. C **71**, 1582 (2011).

[25] Z. G. Wang, Analysis of strong decays of the charmed mesons D(2550), D(2600), D(2750) and D(2760), Phys. Rev. D **83**, 014009 (2011).

[26] Z. G. Wang, Analysis of strong decays of the charmed mesons $D_J(2580)$, $D_J^*(2650)$, $D_J(2740)$, $D_J^*(2760)$, $D_J(3000)$, $D_J^*(3000)$, Phys. Rev. D **88**, 114003 (2013).

[27] E. van Beveren and G. Rupp, Comment on "Study of D_{sJ} decays to D^*K in inclusive e^+e^- interactions", Phys. Rev. D **81**, 118101 (2010).

[28] A. M. Badalian and B. L. G. Bakker, Higher excitations of the D and D_s mesons, Phys. Rev. D **84**, 034006 (2011).

[29] F. E. Close, C. E. Thomas, O. Lakhina, and E. S. Swanson, Canonical interpretation of the $D_{sJ}(2860)$ and $D_{sJ}(2690)$, Phys. Lett. B **647**, 159 (2007).

[30] S. Godfrey and I. T. Jardine, Comment on the nature of the $D_{s1}^*(2710)$ and $D_{sJ}^*(2860)$ mesons, Phys. Rev. D **89**, 074023 (2014).

[31] S. Godfrey and K. Moats, The $D_{sJ}^*(2860)$ mesons as excited D-wave $c\bar{s}$ states, Phys. Rev. D **90**, 117501 (2014); **92**, 119903(E) (2015).

[32] B. Chen, L. Yuan, and A. Zhang, Possible 2S and 1D charmed and charmed-strange mesons, Phys. Rev. D **83**, 114025 (2011).

[33] G. Moir, M. Peardon, S. M. Ryan, C. E. Thomas, and L. Liu, Excited spectroscopy of charmed mesons from lattice QCD, J. High Energy Phys. 05 (2013) 021.

[34] R. Lewis and R. M. Woloshyn, S- and P-wave heavy light mesons in lattice NRQCD, Phys. Rev. D **62**, 114507 (2000).

[35] K. Cichy, M. Kalinowski, and M. Wagner, Mass spectra of mesons containing charm quarks—continuum limit results from twisted mass fermions, *Proc. Sci.*, LATTICE 2015 (2015) 093 [arXiv:1510.07862].

[36] A. De Rujula, H. Georgi, and S. L. Glashow, Charm Spectroscopy via Electron-Positron Annihilation, Phys. Rev. Lett. **37**, 785 (1976).

[37] J. L. Rosner, P-wave mesons with one heavy quark, Comments Nucl. Part. Phys. **16**, 109 (1986).

[38] N. Isgur and M. B. Wise, Spectroscopy with Heavy Quark Symmetry, Phys. Rev. Lett. **66**, 1130 (1991).

[39] E. J. Eichten, C. T. Hill, and C. Quigg, Properties of Orbitally Excited Heavy-Light Mesons, Phys. Rev. Lett. **71**, 4116 (1993).

[40] M. Lu, M. B. Wise, and N. Isgur, Heavy quark symmetry and $D_1(2420) \to D^*\pi$ decay, Phys. Rev. D **45**, 1553 (1992).

[41] S. Godfrey and R. Kokoski, The properties of P-wave mesons with one heavy quark, Phys. Rev. D **43**, 1679 (1991).

[42] S. Godfrey and N. Isgur, Mesons in a relativized quark model with chromodynamics, Phys. Rev. D **32**, 189 (1985).

[43] L. Micu, Decay rates of meson resonances in a quark model, Nucl. Phys. **B10**, 521 (1969).

[44] A. Le Yaouanc, L. Oliver, O. Pene, and J. C. Raynal, Naive quark-pair-creation model of strong interaction vertices, Phys. Rev. D **8**, 2223 (1973).

[45] S. Godfrey, High spin mesons in the quark model, Phys. Rev. D **31**, 2375 (1985).

[46] S. Godfrey and N. Isgur, Isospin violation in mesons and the constituent quark masses, Phys. Rev. D **34**, 899 (1986).

[47] S. Godfrey, Spectroscopy of B_c mesons in the relativized quark model, Phys. Rev. D **70**, 054017 (2004).

[48] S. Godfrey, Properties of the charmed P-wave mesons, Phys. Rev. D **72**, 054029 (2005).

[49] M. Di Pierro and E. Eichten, Excited heavy-light systems and hadronic transitions, Phys. Rev. D **64**, 114004 (2001).

[50] D. Ebert, V. O. Galkin, and R. N. Faustov, Mass spectrum of orbitally and radially excited heavy-light mesons in the relativistic quark model, Phys. Rev. D **57**, 5663 (1998); **59**, 019902(E) (1998).

[51] D. Ebert, R. N. Faustov, and V. O. Galkin, Heavy-light meson spectroscopy and Regge trajectories in the relativistic quark model, Eur. Phys. J. C **66**, 197 (2010).

[52] S. F. Radford, W. W. Repko, and M. J. Saelim, Potential model calculations and predictions for $c\bar{s}$ quarkonia, Phys. Rev. D **80**, 034012 (2009).

[53] M. Shah, B. Patel, and P. C. Vinodkumar, Mass spectra and decay properties of D_s meson in a relativistic Dirac formalism, Phys. Rev. D **90**, 014009 (2014).

[54] S. N. Gupta and J. M. Johnson, Quantum chromodynamic potential model for light heavy quarkonia and the heavy quark effective theory, Phys. Rev. D **51**, 168 (1995).

[55] F. E. Close and E. S. Swanson, Dynamics and decay of heavy-light hadrons, Phys. Rev. D **72**, 094004 (2005).

[56] T. Barnes and S. Godfrey, Charmonium options for the $X(3872)$, Phys. Rev. D **69**, 054008 (2004).

[57] T. Barnes, S. Godfrey, and E. S. Swanson, Higher charmonia, Phys. Rev. D **72**, 054026 (2005).

[58] H. G. Blundell and S. Godfrey, The $\xi(2220)$ reexamined: strong decays of the 1^3F_2 and 1^3F_4 $s\bar{s}$ mesons, Phys. Rev. D **53**, 3700 (1996).

[59] S. Godfrey, Testing the nature of the $D_{sJ}^*(2317)^+$ and $D_{sJ}(2463)^+$ states using radiative transitions, Phys. Lett. B **568**, 254 (2003).

[60] B. Aubert *et al.* (*BABAR* Collaboration), Observation of a Narrow Meson Decaying to $D_s^+\pi^0$ at a Mass of 23.2 GeV/c^2, Phys. Rev. Lett. **90**, 242001 (2003).

[61] P. Krokovny *et al.* (Belle Collaboration), Observation of the $D_{sJ}(2317)$ and $D_{sJ}(2457)$ in B Decays, Phys. Rev. Lett. **91**, 262002 (2003).

[62] S.-K. Choi *et al.* (Belle Collaboration), Observation of a Narrow Charmoniumlike State in Exclusive $B^{\pm} \to K^{\pm}\pi^{+}\pi^{-}J/\psi$ Decays, Phys. Rev. Lett. **91**, 262001 (2003).
[63] S. Godfrey and S. L. Olsen, The exotic XYZ charmonium-like mesons, Annu. Rev. Nucl. Part. Sci. **58**, 51 (2008).
[64] S. Godfrey, in *Proceedings of DPF-2009, Detroit, Michigan, 2009*, edited by P. E. Karchin and A. A Petrov, eConf C090726 (2009).
[65] E. Braaten, in *Proceedings of the 6th International Workshop on Charm Physics (CHARM 2013), Manchester, United Kingdom, 2013*, edited by M. Gersabeck and C. Parkes, eConf C130831 (2013).
[66] F. De Fazio, New spectroscopy of heavy mesons, *Proc. Sci.*, HQL 2012 (2012) 001.
[67] E. J. Eichten, K. Lane, and C. Quigg, Charmonium levels near threshold and the narrow state $X(3872) \to \pi^{+}\pi^{-}J/\psi$, Phys. Rev. D **69**, 094019 (2004).
[68] R. N. Cahn and J. D. Jackson, Spin orbit and tensor forces in heavy quark light quark mesons: implications of the new D_s state at 2.32 GeV, Phys. Rev. D **68**, 037502 (2003).
[69] E. J. Eichten and C. Quigg, Mesons with beauty and charm: spectroscopy, Phys. Rev. D **49**, 5845 (1994).
[70] This is discussed more fully in Appendix A of T. Barnes, N. Black, and P. R. Page, Strong decays of strange quarkonia, Phys. Rev. D **68**, 054014 (2003).
[71] See for example W. Kwong and J. L. Rosner, D-wave quarkonium levels of the upsilon family, Phys. Rev. D **38**, 279 (1988).
[72] A. J. Siegert, Note on the interaction between nuclei and electromagnetic radiation, Phys. Rev. **52**, 787 (1937).
[73] R. McClary and N. Byers, Relativistic effects in heavy quarkonium spectroscopy, Phys. Rev. D **28**, 1692 (1983).
[74] P. Moxhay and J. L. Rosner, Relativistic corrections in quarkonium, Phys. Rev. D **28**, 1132 (1983).
[75] J. D. Jackson, in *Proceedings of the Summer Institute on Particle Physics, August 2–13, 1976*, edited by M. C. Zipf (Stanford Linear Accelerator Center Report No. SLAC-198, 1977), p. 147.
[76] V. A. Novikov, L. B. Okun, M. A. Shifman, A. I. Vainshtein, M. B. Voloshin, and V. I. Zakharov, Charmonium and gluons, Phys. Rep. **41C**, 1 (1978).
[77] This expression for the decay width comes from E. Swanson (private communication).
[78] Relativistic effects in M1 transitions are discussed in J. S. Kang and J. Sucher, Radiative M1 transitions of the narrow resonances, Phys. Rev. D **18**, 2698 (1978); H. Grotch and K. J. Sebastian, Magnetic dipole transitions of narrow resonances, Phys. Rev. D **25**, 2944 (1982); V. Zambetakis and N. Byers, Magnetic dipole transitions in quarkonia, Phys. Rev. D **28**, 2908 (1983); H. Grotch, D. A. Owen, and K. J. Sebastian, Relativistic corrections to radiative transitions and spectra of quarkonia, Phys. Rev. D **30**, 1924 (1984); X. Zhang, K. J. Sebastian, and H. Grotch, M1 decay rates of heavy quarkonia with a nonsingular potential, Phys. Rev. D **44**, 1606 (1991).
[79] See Supplemental Material at http://link.aps.org/supplemental/10.1103/PhysRevD.93.034035 for detailed tables of our calculated decay widths, branching ratios and electromagnetic transition matrix elements.
[80] E. S. Ackleh, T. Barnes, and E. S. Swanson, On the mechanism of open flavor strong decays, Phys. Rev. D **54**, 6811 (1996).
[81] Z. F. Sun and X. Liu, Newly observed $D_{sJ}(3040)$ and the radial excitations of P-wave charmed-strange mesons, Phys. Rev. D **80**, 074037 (2009).
[82] J. Ferretti and E. Santopinto, Open-flavor strong decays of open-charm and open-bottom mesons in the $^3P_0$ pair-creation model, arXiv:1506.04415.
[83] P. Colangelo, F. De Fazio, F. Giannuzzi, and S. Nicotri, New meson spectroscopy with open charm and beauty, Phys. Rev. D **86**, 054024 (2012).
[84] X.-H. Zhong and Q. Zhao, Strong decays of newly observed D_{sJ} states in a constituent quark model with effective Lagrangians, Phys. Rev. D **81**, 014031 (2010).
[85] X.-H. Zhong and Q. Zhao, Strong decays of heavy-light mesons in a chiral quark model, Phys. Rev. D **78**, 014029 (2008).
[86] S. Godfrey and K. Moats, Bottomonium mesons and strategies for their observation, Phys. Rev. D **92**, 054034 (2015).
[87] R. Kokoski and N. Isgur, Meson decays by flux tube breaking, Phys. Rev. D **35**, 907 (1987).
[88] H. G. Blundell, S. Godfrey, and B. Phelps, Properties of the strange axial mesons in the relativized quark model, Phys. Rev. D **53**, 3712 (1996).
[89] J. Ferretti and E. Santopinto, Higher mass bottomonia, Phys. Rev. D **90**, 094022 (2014).
[90] J. Segovia, D. R. Entem, and E. Fernandez, Scaling of the $^3P_0$ strength in heavy meson decays, Phys. Lett. B **715**, 322 (2012).
[91] Q. F. Lü and D. M. Li, Understanding the charmed states recently observed by the LHCb and *BABAR* collaborations in the quark model, Phys. Rev. D **90**, 054024 (2014).
[92] E. van Beveren and G. Rupp, $D_{sJ}(2860)$ as the First Radial Excitation of the $D^*_{s0}(2317)$, Phys. Rev. Lett. **97**, 202001 (2006).
[93] A. Zhang, Implications to $\bar{c}s$ assignments of $D_{s1}(2700)^{\pm}$ and $D_{sJ}(2860)$, Nucl. Phys. **A856**, 88 (2011).
[94] B. Chen, D.-X. Wang, and A. Zhang, Interpretation of $D_{sJ}(2632)^{+}$, $D_{s1}(2700)^{\pm}$, $D^*_{sJ}(2860)^{+}$ and $D_{sJ}(3040)^{+}$, Phys. Rev. D **80**, 071502 (2009).
[95] D.-M. Li and B. Ma, Implication of *BABAR*'s new data on the $D_{s1}(2710)$ and $D_{sJ}(2860)$, Phys. Rev. D **81**, 014021 (2010).
[96] G.-L. Wang, Y. Jiang, T. Wang, and W.-L. Ju, The properties of $D^*_{s1}(2700)^{+}$, arXiv:1305.4756.
[97] B. Chen, X. Liu, and A. Zhang, A combined study of $2S$ and $1D$ open-charm mesons with natural spin parity, Phys. Rev. D **92**, 034005 (2015).
[98] X. H. Zhong, Strong decays of the newly observed $D(2550)$, $D(2600)$, $D(2750)$, and $D(2760)$, Phys. Rev. D **82**, 114014 (2010).
[99] L. Yuan, B. Chen, and A. Zhang, $D^{\star}_{s1}(2700)^{\pm}$ and $D^{\star}_{sJ}(2860)^{\pm}$ revisited within the $^3P_0$ Model, arXiv:1203.0370.
[100] P. Colangelo and F. De Fazio, Open charm meson spectroscopy: where to place the latest piece of the puzzle, Phys. Rev. D **81**, 094001 (2010).